Private versus Social Responses to a Pandemic

Miguel Casares*and Paul Gomme†and Hashmat Khan‡

June 18, 2024

Abstract

What are the socially optimal restrictions on private activity during a pandemic? How do these differ from private decisions? We address these questions by modeling the interactions between epidemiology and the macroeconomy. Unlike the private planner, the social planner accounts for two externalities: the increase in the cost of severe illness associated with more infected individuals, reflecting the capacity constraints of the health care system; and the socioeconomic transmission of the virus from asymptomatic to susceptible individuals. Owing to these externalities, the social planner imposes stricter constraints on socioeconomic activities. Applied to the COVID-19 pandemic, socially optimal restrictions reduce the welfare costs by roughly one percent of GDP.

Keywords: epi-macro, socioeconomic contacts, externality
JEL Codes: I18, E61, E13, E11

*Universidad Pública de Navarra and Barnard College. mcasares@unavarra.es, https://sites.google.com/unavarra.es/mcasares. Financial support from the Spanish government (research project PID2021-127119NB-I00) is acknowledged.

†Concordia University, CIREQ and CIRANO. paul.gomme@concordia.ca, https://paulgomme.github.io/. Financial support was gratefully received from the Social Sciences and Humanities Research Council (Canada) Grant Number 435–2016–1388.

‡Carleton University. hashmat.khan@carleton.ca, https://carleton.ca/khan/

1 Introduction

Public policy responses to the pandemics vary widely. For example, during the SARS-CoV-2/COVID-19 pandemic, some jurisdictions strictly limited socioeconomic activity while others took a more laissez-faire approach. No doubt policymakers receive conflicting recommendations with advisors more concerned about public health advocating for fairly strict measures, and those worried about the economy pushing for more leniency. The question addressed in this paper is: Balancing the health and socioeconomic costs, what *should* the public policy response to a pandemic be? We answer this question by solving the social planner problem for a tractable model of the interactions between epidemiology and economic decisions. The presence of externalities, described shortly, differentiate the social and private responses to the pandemic. In brief, the social optimum sees less socioeconomic activity than the private optimum.

The recent pandemic spawned a vast literature incorporating epidemiology into macroeconomic models. While this literature predominantly uses a SIR (susceptible-infected-recovered) epidemiological model, we develop a SAIS (susceptible-asymptomatic-infected-susceptible) model. This choice is motivated by the recent pandemic in which SARS-CoV-2 reinfections are commonplace, a fact that the SIR model cannot account for since the recovered enjoy permanent immunity. From a public policy perspective, an important difference between SIR and SIS models (and their variants) is that in a SIR environment, the problem is managing the transition to the end of the pandemic when "herd immunity" is achieved whereas, in SIS environments one must manage both the initial pandemic and the eventual endemic. Further, given that the virus transmission often involves those without symptoms, distinguishing between asymptomatic and infected (meaning those *with* symptoms) is important. To capture the rapid pace of an illness, a model period is a day. Within the model, the only observable distinction between individuals is whether they are (*known* to be) infected or not. In other words, susceptible and asymptomatic individuals are observationally equivalent, and so are treated the same. The probability that a susceptible individual becomes asymptomatic depends on three factors: the likelihood of encountering an asymptomatic individual, the per-contact probability of contracting the virus in such an encounter, and the number of daily contacts.

The macroeconomic side of the model builds on the neoclassical growth model. In the interests of tractability, the model consists of a continuum of families, each composed of a continuum of family members; this feature has been employed within the unemployment literature. Non-infected (susceptible and asymptomatic) family members work, socialize and consume, all of which determine their number of daily contacts. As discussed above, daily

contacts are a key determinant that a susceptible individual contracts the virus, thereby becoming asymptomatic. Known infected family members self isolate in such a way as to generate no daily contacts: they consume but do not work, and minimize their social interactions. The large family construct is convenient for the following reasons. First, savings occur at the family level; there is no within-family wealth distribution. Second, the family provides insurance to its members; in particular, it takes care of (known) infected members while they isolate. These insurance flows stand in for the myriad public policies aimed at mitigating the economic costs of a pandemic. Third, with a continuum of family members, the law of large numbers implies that the measure of family members by epidemiological status is known, even though the status of a given non-infected member is not.

Two externalities motivate the distinction between decisions made by a private planner operating at the level of the family, and a social planner making aggregate-level decisions. The first is the *transmission externality*. As previously discussed, the probability that a susceptible individual catches the virus depends in part on the likelihood of encountering an asymptomatic individual. In choosing daily contacts, the private planner only takes into consideration the probability that its *own* susceptible family members catch the virus, taking as given the probability of encountering an asymptomatic. In addition, the social planner accounts for how the distribution of the population across the various health states affects the probability of meeting with an asymptomatic. The second is a *cost externality*. In addition to the restrictions associated with self isolation, (known) infected individuals suffer a daily utility loss of being sick with severe illness. To capture the effects of health care congestion and capacity constraints, this daily cost is increasing in the total number of infected individuals. Only the social planner accounts for how the aggregate measure of infected people affects the daily cost of being infected.

The pandemic spawned a great number of papers combining macroeconomics and epidemiology with notable early contributions by Atkeson (2020) and Eichenbaum, Rebelo, and Trabandt (2021). Rather than try to summarize this vast literature, the interested reader is directed to the scoping review of Bonnet et al. (2024). Almost all of the 80 papers reviewed use some variant of the SIR epidemiological model which, as discussed above, does not characterize the reinfections that occur with COVID-19.

Gainnitsarou, Kissler, and Toxvaerd (2021) is one of the few papers using some form of SIS model as we do. They focus on the socially optimal response to the pandemic while we characterize the differences between the privately and socially optimal responses. As well, the macroeconomic side of our model is a more traditional neoclassical model, and we include the intensity of contacts in the contagion probability.

The model is laid out in Section 2. The calibration in Section 3 is disciplined using obser-

vations for the SARS-CoV-2/COVID-19 pandemic. Properties of steady state are explored in Section 4. The main results are presented in Section 5 which compares the responses of the private and social planners to the start of a pandemic. Section 6 gives advice for how to handle a new variant of concern. We discuss some possible extensions in Section 7, and wrap up the paper with some concluding remarks in Section 8.

2 The Macroeconomic-Epidemiological Model

2.1 Epidemiology

As discussed in the introduction, the appropriate model for studying a pandemic with reinfections, like COVID-19, is a SAIS model in which individuals transition from susceptible (S) to asymptomatic (A) to infected (I) then back to susceptible (S) and so liable to reinfection. Asymptomatics are included in the model owing to the observation that there is often a latent phase during which individuals show no symptoms, and can unknowingly spread the disease. Those known to be infected are assumed to self isolate. Without asymptomatics, the model's pandemic would be very short lived. Throughout, we use the term "infected" to mean those who have clear, severe symptoms. Those who are "infected" are distinct from "asymptomatics" who have caught the virus but have yet to display symptoms. This definition "infected" differs from its colloquial meaning of contracting a disease. In order to capture the relatively short period of time spent in both the asymptomatic and infected stages of the disease, a model period needs to be short; we set it to a day.

The susceptible group is further divided into those with low, medium and high infection probabilities. The low infection probability type is included to capture the fact that those who have recently recovered enjoy a temporary anti-body boost making them, for a while, less likely to catch the virus again. In order to study the model's predictions for the effects of both the initial phases of a pandemic as well as a new, more contagious virus variant, a high infection probability type is incorporated into the model. One way of thinking about this is that those who have been through a past illness have some degree of immunity to the currently prevalent variant, but not to a new variant.

Not everyone who contracts the virus displays definite symptoms, and cases differ in their severity. With this in mind, the asymptomatic group is subdivided in two. The first group eventually experiences severe symptoms at which point they are (known) infected. This first group will be referred to as asymptomatic-infected. The second group has such a mild case that they effectively bypasses the infected state; they will be referred to as asymptomatic-susceptible since, upon recovery, they are susceptible with a low infection probability. Those

passing through the infected state likewise exit to the susceptible pool with a low infection probability.

Figure 1: Epidemiological Flows

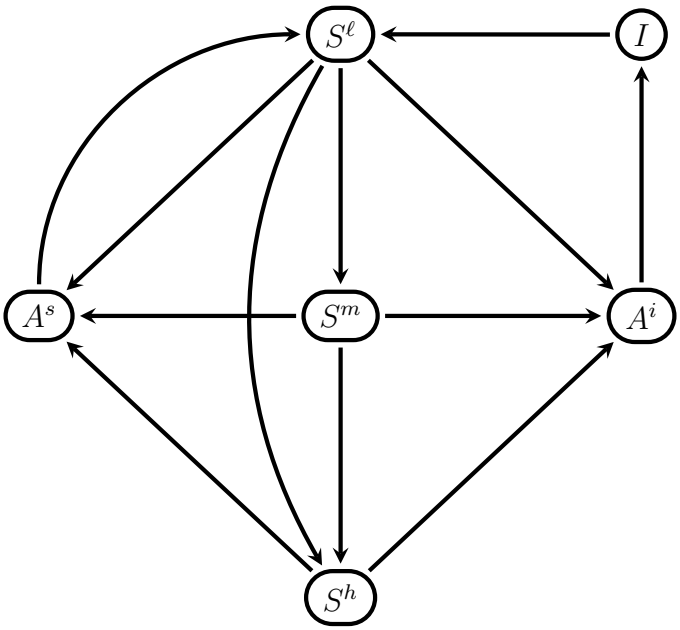

To better understand the epidemiological part of the model, as summarized by Fig. 1, consider someone who has just contracted the virus. They are initially asymptomatic, and may be in the mild group, A^s, where the superscript indicates the pool to which they will exit. Alternatively, they may be in the severely sick group, A^i, eventually exiting to the (known) infected group (denoted I). All of those recovering from illness, the A^s and I groups, become susceptible with a low infection probability, S^ℓ, reflecting the temporary immunity boost from recently recovering from the disease. Over time, this immunity boost is lost and the individual becomes susceptible with a medium infection probability, S^m. Individuals' immunity to a new variant is lower than the prevailing variant. To capture this phenomena, both low and medium infection probability susceptibles may suddenly be susceptible with a high infection probability, S^h. To close the circle, all susceptibles face some likelihood of contracting the virus and become one of the asymptomatics, albeit with differing probabilities of infection.

Consistent with the flows depicted in Fig. 1, movements between these epidemiological states are determined by transition probabilities. Think of an individual's epidemiological status as being determined over night. For someone who goes to bed as a susceptible: first, they may become asymptomatic; if not, then second, their infection likelihood may increase.

For an asymptomatic, they either stay as they are, or become susceptible-low (in the case of mild cases) or become infected (severe cases). Likewise, the infected recover with some probability, becoming susceptible with a low likelihood of (re)infection. The dynamics of population measures are:

$$N_{t+1}^{s\ell} = (1-P_t^{\ell})(1-\nu^{s\ell,sh})(1-\nu^{s\ell,sm})N_t^{s\ell} + \nu^{as,s\ell}N_t^{as} + \nu^{i,s\ell}N_t^{i} \tag{1}$$

$$N_{t+1}^{sm} = (1-P_t^{m})(1-\nu^{sm,sh})N_t^{sm} + (1-P_t^{\ell})(1-\nu^{s\ell,sh})\nu^{s\ell,sm}N_t^{s\ell} \tag{2}$$

$$N_{t+1}^{sh} = (1-P_t^{h})N_t^{sh} + (1-P_t^{\ell})\nu^{s\ell,sh}N_t^{s\ell} + (1-P_t^{m})\nu^{sm,sh}N_t^{sm} \tag{3}$$

$$N_{t+1}^{as} = (1-\nu^{as,s\ell})N_t^{as} + P_t^{\ell}\nu^{s\ell,as}N_t^{s\ell} + P_t^{m}\nu^{sm,as}N_t^{sm} + P_t^{h}\nu^{sh,as}N_t^{sh} \tag{4}$$

$$N_{t+1}^{ai} = (1-\nu^{ai,i})N_t^{ai} + P_t^{\ell}\nu^{s\ell,ai}N_t^{s\ell} + P_t^{m}\nu^{sm,ai}N_t^{sm} + P_t^{h}\nu^{sh,ai}N_t^{sh} \tag{5}$$

$$N_{t+1}^{i} = (1-\nu^{i,s\ell})N_t^{i} + \nu^{ai,i}N_t^{ai}. \tag{6}$$

P_t^j is the endogenous probability that a type-j ($j \in \{\ell, m, h\}$) susceptible catches the virus; $\nu^{j,k}$, are the exogenous probability that a type j becomes a type k ($j, k \in \{s\ell, sm, sh, as, ai, i\}$). Writing the vector of population measures,

$$N_t = [N_t^{s\ell},\ N_t^{sm},\ N_t^{sh},\ N_t^{as},\ N_t^{ai},\ N_t^{i}]^T \tag{7}$$

these dynamics can be written more succinctly as

$$N_{t+1} = \Pi_t N_t \tag{8}$$

where Π_t is the (Markov) transition matrix:

$$\begin{bmatrix}
(1-P_t^{\ell})(1-\nu^{s\ell,sh})(1-\nu^{s\ell,sm}) & 0 & 0 & \nu^{as,s\ell} & 0 & \nu^{i,s\ell} \\
(1-P_t^{\ell})(1-\nu^{s\ell,sh})\nu^{s\ell,sm} & (1-P_t^{m})(1-\nu^{sm,sh}) & 0 & 0 & 0 & 0 \\
(1-P_t^{\ell})\nu^{s\ell,sh} & (1-P_t^{m})\nu^{sm,sh} & 1-P_t^{h} & 0 & 0 & 0 \\
P_t^{l}\nu^{s\ell,as} & P_t^{m}\nu^{sm,as} & P_t^{h}\nu^{sh,as} & 1-\nu^{as,s\ell} & 0 & 0 \\
P_t^{l}\nu^{s\ell,ai} & P_t^{m}\nu^{sm,ai} & P_t^{h}\nu^{sh,ai} & 0 & 1-\nu^{ai,i} & 0 \\
0 & 0 & 0 & 0 & \nu^{ai,i} & 1-\nu^{i,s\ell}
\end{bmatrix} \tag{9}$$

What do individuals know about their epidemiological status? Only whether they are infected, or not. Susceptible and asymptomatics only know that they are not currently infected. Dividing the susceptibles into groups based on their infection probability, and asymptomatics by the eventual severity of their infection is an accounting device in the model. It is this 'not knowing' that allows asymptomatics to circulate in the socioeconomic environment with a clear conscience.

2.2 The Private Planner

For tractability, we model individual behavior as arising from decisions made by a private planner. There are a continuum on the unit interval of families, each comprised of a continuum on the unit interval of family members. Throughout, lowercase letters denote private planner (household-level) variables while uppercase letters are used for aggregate and social planner-specific variables.

Each day, a family member receives utility from consumption, leisure, and time spent on socialization. The private family planner cares equally about all family members and directs their activity. As discussed above, the only distinction between individuals is whether or not they are infected. Consequently, the planner sends out separate instructions to those who are infected, and those who are not. The infected are told to self isolate; they do not work ($h_t^i = 0$), they minimize their socializing time to $\underline{s}$, and they are optimally allocated a level of consumption c_t^i. Since each family member has a unit endowment of time, leisure of the infected is $\ell_t^i = 1 - \underline{s}$. Daily utility of an infected family member is $U(c_t^i, 1 - \underline{s}, \underline{s}) - L(N_t^i)$ where $L(N_t^i) = \xi_1 + \xi_2 (N_t^i)^{\xi_3}$ is the daily disutility of severe illness which captures the value of social isolation, misery, and proxies for death. The specific functional for L is increasing and convex in the *population* measure of infected individuals, N_t^i, capturing the fact that hospital capacity constraints affect an individual's treatment options. This is the infection *cost externality*.

The remaining family members are issued instructions to work h_t, socialize s_t and consume c_t. Their daily utility is $U(c_t, \ell_t, s_t)$ where leisure is $\ell_t = 1 - h_t - s_t$ and

$$U(c, \ell, s) = \ln c + \omega \ln \ell + \phi \ln s, \quad \phi, \omega > 0. \tag{10}$$

In going about this socioeconomic activity, an individual generates daily contacts,

$$y_t = \mu_c c_t + \mu_h h_t + \mu_s s_t \tag{11}$$

where μ_c, μ_h and μ_s are scaling parameters which will be calibrated so that daily contacts by source match the data. Specifically, daily contacts result from consumption (shopping), work, and socialization. The relevance of these daily contacts is that they determine infection probabilities. In a meeting with an asymptomatic, a type j susceptible will catch the virus with type-specific probability α^j, $j \in \{\ell, m, h\}$. The frequency of meeting an asymptomatic in a daily contact is

$$F_t = \frac{(N_t^{as} + N_t^{ai}) Y_t}{(N_t^{s\ell} + N_t^{sm} + N_t^{sh} + N_t^{as} + N_t^{ai}) Y_t}$$

$$= \frac{N_t^{as} + N_t^{ai}}{N_t^{s\ell} + N_t^{sm} + N_t^{sh} + N_t^{as} + N_t^{ai}}. \tag{12}$$

Since the non-infection probability in a given meeting is $1-\alpha^j F_t$, engaging in y_t daily contacts leads to the daily infection probability of a type j susceptible:

$$P_t^j = P(y_t, F_t; \alpha^j) = 1 - (1 - \alpha^j F_t)^{y_t}, \quad j \in \{\ell, m, h\}. \tag{13}$$

The effect of a change in personal daily contacts, y_t, on the infection probability is

$$\frac{\partial P_t^j}{\partial y_t} = -(1 - \alpha^j F_t)^{y_t} \ln(1 - \alpha^j F_t) > 0, \quad j \in \{\ell, m, h\}. \tag{14}$$

Since $\alpha^j \in (0,1)$, and since $\ln x < 0$ for $0 < x < 1$, it follows that the partial derivative in (14) is positive: more daily contacts increases the probability that susceptible family members transition to asymptomatic.

While the private planner does not know the epidemiological status of a given non-infected family member, by the law of large numbers the private planner nonetheless knows the measures of family members by epidemiological status. Consequently, the private planner sends family members into the socioeconomic environment *knowing* that some are susceptible and will return having contracted the virus. The planner further knows that other family members are asymptomatic and will infect susceptible members of other families. However, since the family is small relative to the population, the private planner does not account how their choices for family members affects the aggregate probability of contracting the virus: $\frac{\partial P_t^j}{\partial n_t^k} = 0$ for $j \in \{\ell, m, h\}$ and $k \in \{s\ell, sm, sh, as, ai\}$. At the aggregate level, the measures by epidemiological status do affect this virus-contracting probability, reflecting the virus *transmission externality* which is not accounted for by the family planner.

The private planner's Bellman equation is

$$\begin{aligned} V(a_t, n_t^{s\ell}, n_t^{sm}, n_t^{sh}, n_t^{as}, n_t^{ai}, n_t^i; \mathcal{S}_t) \equiv \max\Big\{ & (n_t^{s\ell} + n_t^{sm} + n_t^{sh} + n_t^{as} + n_t^{ai}) U(c_t, \ell_t, s_t) \\ & + n_t^i [U(c_t^i, 1 - \underline{s}, \underline{s}) - L(N_t^i)] + \beta V(a_{t+1}, n_{t+1}^{s\ell}, n_{t+1}^{sm}, n_{t+1}^{sh}, n_{t+1}^{as}, n_{t+1}^{ai}, n_{t+1}^i; \mathcal{S}_{t+1}) \\ & + \lambda_t \big[w_t (n_t^{s\ell} + n_t^{sm} + n_t^{sh} + n_t^{as} + n_t^{ai}) h_t + R_t^k a_t \\ & \quad - (n_t^{s\ell} + n_t^{sm} + n_t^{sh} + n_t^{as} + n_t^{ai}) c_t - n_t^i c_t^i - a_{t+1} \big] \\ & + \left[n_t^T \Pi_t^T - n_{t+1}^T \right] \Lambda_t \Big\} \end{aligned} \tag{15}$$

with

$$y_t = \mu_c c_t + \mu_h h_t + \mu_s s_t, \tag{16}$$

$$\ell_t = 1 - h_t - s_t \tag{17}$$

Above, w_t is the real wage; $R_t^k = r_t + 1 - \delta$ is the gross return to assets (capital) with r_t being the rental rate for capital and $\delta \in [0,1]$ the depreciation rate; Λ_t is a vector of Lagrange multipliers attached to the law of motion for family members by epidemiological status; and $\mathcal{S}_t$ is a vector of aggregate state variables.

The private planner's Euler equations are:

$$c_t: \quad (1 - n_t^i)\left[U_1(c_t, \ell_t, s_t) - \lambda_t\right] + \mu_c n_t^T \frac{\partial \Pi_t^T}{\partial y_t} \Lambda_t = 0 \tag{18}$$

$$c_t^i: \quad U_1(c_t^i, 1 - \underline{s}, \underline{s}) - \lambda_t = 0 \tag{19}$$

$$h_t: \quad (1 - n_t^i)\left[\lambda_t w_t - U_2(c_t, \ell_t, s_t)\right] + \mu_h n_t^T \frac{\partial \Pi_t^T}{\partial y_t} \Lambda_t = 0 \tag{20}$$

$$s_t: \quad (1 - n_t^i)\left[U_3(c_t, \ell_t, s_t) - U_2(c_t, \ell_t, s_t)\right] + \mu_s n_t^T \frac{\partial \Pi_t^T}{\partial y_t} \Lambda_t = 0 \tag{21}$$

$$a_{t+1}: \quad \lambda_t = \beta \lambda_{t+1} R_{t+1}^k \tag{22}$$

$$n_{t+1}: \quad \Lambda_t = \beta \left\{ \begin{bmatrix} U(c_{t+1}, \ell_{t+1}, s_{t+1}) \\ U(c_{t+1}, \ell_{t+1}, s_{t+1}) \\ U(c_{t+1}, \ell_{t+1}, s_{t+1}) \\ U(c_{t+1}, \ell_{t+1}, s_{t+1}) \\ U(c_{t+1}, \ell_{t+1}, s_{t+1}) \\ U(c_{t+1}^i, 1 - \underline{s}, \underline{s}) - L(N_t^i) \end{bmatrix} + \lambda_{t+1} \begin{bmatrix} w_{t+1} h_{t+1} - c_{t+1} \\ w_{t+1} h_{t+1} - c_{t+1} \\ w_{t+1} h_{t+1} - c_{t+1} \\ w_{t+1} h_{t+1} - c_{t+1} \\ w_{t+1} h_{t+1} - c_{t+1} \\ -c_{t+1}^i \end{bmatrix} + \Pi_{t+1}^T \Lambda_{t+1} \right\} \tag{23}$$

In interpreting (23), start by noting that the vector of Lagrange multipliers, Λ_t, are the shadow values of family members by epidemiological status at the end of day t. These values are determined by: (a) the direct utility contribution of each epidemiological type; in the case of infected members, net of the utility cost of being sick, $L(N_t^i)$; (b) the utility value of each type's net contribution to family resources, their labor income (in the case of non-infected members) less their consumption; and (c) the shadow values of family member types after accounting for the various possible transitions.

Compare (18), (20) and (21) with their non-pandemic counterparts,

$$c_t: \quad U_1(c_t, \ell_t, s_t) = \lambda_t \tag{24}$$

$$h_t: \quad U_2(c_t, \ell_t, s_t) = \lambda_t w_t \tag{25}$$

$$s_t: \quad U_3(c_t, \ell_t, s_t) = U_2(c_t, \ell_t, s_t) \tag{26}$$

The key difference is the capital loss associated with an increase in daily contacts, the

pandemic wedge,

$$\mathcal{W}_t^p = n_t^T \frac{\partial \Pi_t^T}{\partial y_t} \Lambda_t \tag{27}$$

$$\begin{aligned} =& \Big[\nu^{s\ell,as}\Lambda_t^{as} + \nu^{s\ell,ai}\Lambda_t^{ai} - (1-\nu_t^{s\ell,sh})(1-\nu^{s\ell,sm})\Lambda_t^{s\ell} \\ & - (1-\nu_t^{s\ell,sh})\nu^{s\ell,sm}\Lambda_t^{sm} - \nu_t^{s\ell,sh}\Lambda_t^{sh}\Big]\frac{\partial P_t^{\ell}}{\partial y_t} n_t^{s\ell} \\ & + \left[\nu^{sm,as}\Lambda_t^{as} + \nu^{sm,ai}\Lambda_t^{ai} - (1-\nu_t^{sm,sh})\Lambda_t^{sm} - \nu_t^{sm,sh}\Lambda_t^{sh}\right]\frac{\partial P_t^{m}}{\partial y_t} n_t^{sm} \\ & + \left[\nu^{sh,as}\Lambda_t^{as} + \nu^{sh,ai}\Lambda_t^{ai} - \Lambda_t^{sh}\right]\frac{\partial P_t^{h}}{\partial y_t} n_t^{sh} \end{aligned} \tag{28}$$

Another daily contact increases the probability that a susceptible individual will catch the virus, becoming asymptomatic ($\partial P_t^j/\partial y_t,\ j \in \{\ell, m, h\}$)). Given the large family setup, the planner knows the measure of individuals making transitions from all three susceptible types to both asymptomatic types. Associated with each such transition is a capital loss given by the shadow value of a susceptible less the shadow value of an asymptomatic (the terms in square brackets in (28)). The pandemic wedge is the sum of these three capital losses. Through (18), (20) and (21), this negative pandemic wedge leads the private planner to choose less consumption, fewer hours worked, and less socialization. In analyzing the response of the private planner to the presence of the virus, for example, the size of this wedge governs the magnitude of the adjustments in the private planner's socioeconomic choices.

Inspecting (18) and (19), one can see that the private planner provides consumption insurance to its infected members. This condition is related to the full consumption insurance found in family models of unemployment. However, as above, the pandemic wedge gets in the way of complete consumption insurance. A negative pandemic wedge implies that the marginal utility of the non-infected is higher than that of the infected (full insurance would equalize these marginal utilities), due to the expected capital losses associated with susceptible family members contracting the virus. When preferences are additively separable, infected family members consume more than other family members.

2.3 The Social Planning Problem

The key difference between the private and social planners is that the social planner takes into account the epidemiological externalities while the private planner does not. Specifically, when the private planner chooses socioeconomic activity for its non-infected members, the fact that these choices affect the likelihood that members of *other* families will catch the

virus is not taken into account; the social planner takes on board these externalities. The social planner's Bellman equation is identical to that of the private planner except that the social planner works at the level of the aggregate economy. Importantly, this difference implies that the derivatives of the infection probabilities are now

$$\frac{\partial P_t^j}{\partial N_t^k} = \alpha^j Y_t (1-\alpha^j F_t)^{Y_t - 1} \frac{\partial F_t}{\partial N_t^k}, \quad k \in \{s\ell, sm, sh, as, ai\}, \quad j \in \{\ell, m, h\}, \tag{29}$$

where

$$\frac{\partial F_t}{\partial N_t^k} = \begin{cases} -\frac{N_t^{as}+N_t^{ai}}{(N_t^{s\ell}+N_t^{sm}+N_t^{sh}+N_t^{as}+N_t^{ai})^2} & \text{if } k = s\ell, sm, sh \\ \frac{N_t^{s\ell}+N_t^{sm}+N_t^{sh}}{(N_t^{s\ell}+N_t^{sm}+N_t^{sh}+N_t^{as}+N_t^{ai})^2} & \text{if } k = as, ai \end{cases} \tag{30}$$

respectively, as implied by (12) and (13) with Y_t replacing y_t. Notice that more susceptibles lower the probability that a given meeting is with an asymptomatic while more asymptomatics raise this likelihood.

Apart from the differences in notation (family member variables indicated by lower case, social planner variables by upper case), the two planner's Bellman equations are the same, as are the Euler equations with the exception that (23) is replaced by:

$$\begin{aligned} \Lambda_t = \beta \Bigg\{ & \begin{bmatrix} U(C_{t+1}, L_{t+1}, S_{t+1}) \\ U(C_{t+1}, L_{t+1}, S_{t+1}) \\ U(C_{t+1}, L_{t+1}, S_{t+1}) \\ U(C_{t+1}, L_{t+1}, S_{t+1}) \\ U(C_{t+1}, L_{t+1}, S_{t+1}) \\ U(C_{t+1}^i, 1-\underline{s}, \underline{s}) - L(N_t^i) - N_t^i L'(N_t^i) \end{bmatrix} \\ & + \lambda_{t+1} \begin{bmatrix} w_{t+1}H_{t+1} - C_{t+1} \\ w_{t+1}H_{t+1} - C_{t+1} \\ w_{t+1}H_{t+1} - C_{t+1} \\ w_{t+1}H_{t+1} - C_{t+1} \\ w_{t+1}H_{t+1} - C_{t+1} \\ -C_{t+1}^i \end{bmatrix} + \Pi_{t+1}^T \Lambda_{t+1} + \begin{bmatrix} N_{t+1}^T \frac{\partial \Pi_{t+1}^T}{\partial N_{t+1}^{s\ell}} \Lambda_{t+1} \\ N_{t+1}^T \frac{\partial \Pi_{t+1}^T}{\partial N_{t+1}^{sm}} \Lambda_{t+1} \\ N_{t+1}^T \frac{\partial \Pi_{t+1}^T}{\partial N_{t+1}^{sh}} \Lambda_{t+1} \\ N_{t+1}^T \frac{\partial \Pi_{t+1}^T}{\partial N_{t+1}^{as}} \Lambda_{t+1} \\ N_{t+1}^T \frac{\partial \Pi_{t+1}^T}{\partial N_{t+1}^{ai}} \Lambda_{t+1} \\ N_{t+1}^T \frac{\partial \Pi_{t+1}^T}{\partial N_{t+1}^{i}} \Lambda_{t+1} \end{bmatrix} \Bigg\}. \end{aligned} \tag{31}$$

There are two differences relative to the private planner's corresponding Euler equation. First, the social planner accounts for the cost externality: the increase in the utility cost of severe illness associated with an increase in the population measure of infected individuals, $N_t^i L'(N_t^i)$. Second, the final term in (31) constitutes a new set of wedges which encapsulate the effects of the transmission externality in the model. Take the first term, $N_{t+1}^T \frac{\partial \Pi_{t+1}^T}{\partial N_{t+1}^{s\ell}} \Lambda_{t+1}$,

for example. From (12), an additional susceptible with a low infection probability makes it less likely that any given contact is with an asymptomatic individual (lowers F_t) which, consequently, lowers the probability that any of the susceptible types will contract the virus (P_t^{ℓ}, P_t^{m} and P_t^{h}), thereby becoming asymptomatic. This is the effect captured by the partial derivative, $\frac{\partial \Pi_{t+1}^{T}}{\partial N_{t+1}^{s\ell}}$. Λ_{t+1} is, again, the shadow (utility) value of types, and N_{t+1} their measure. Overall, this term captures the societal capital gain from having an additional susceptible-low type, with this gain operating through its effect on the measures of types and their values.

Due to the symmetric fashion in which the three susceptible types enter the contact-frequency equation, (12), the first three elements in the final column vector in (31) are identical as a consequence of (29) and (30). We will subsequently refer to these wedges,

$$\mathcal{W}_{t+1}^{s} = N_{t+1}^{T} \frac{\partial \Pi_{t+1}^{T}}{\partial N_{t+1}^{k}} \Lambda_{t+1}, \quad k = \{s\ell, sm, sh\} \tag{32}$$

$$\begin{aligned} =& \Big[\nu^{s\ell,as} \Lambda_{t+1}^{as} + \nu^{s\ell,ai} \Lambda_{t+1}^{ai} - (1 - \nu_{t+1}^{s\ell,sh})(1 - \nu^{s\ell,sm}) \Lambda_{t+1}^{s\ell} \\ & - (1 - \nu_{t+1}^{s\ell,sh}) \nu^{s\ell,sm} \Lambda_{t+1}^{sm} - \nu_{t+1}^{s\ell,sh} \Lambda_{t+1}^{sh} \Big] N_{t+1}^{s\ell} \frac{\partial P_{t+1}^{\ell}}{\partial N_{t+1}^{k}} \\ & + \left[\nu^{sm,as} \Lambda_{t+1}^{as} + \nu^{sm,ai} \Lambda_{t+1}^{ai} - (1 - \nu_{t+1}^{sm,sh}) \Lambda_{t+1}^{sm} - \nu_{t+1}^{sm,sh} \Lambda_{t+1}^{sh} \right] N_{t+1}^{sm} \frac{\partial P_{t+1}^{m}}{\partial N_{t+1}^{k}} \\ & + \left[\nu^{sh,as} \Lambda_{t+1}^{as} + \nu^{sh,ai} \Lambda_{t+1}^{ai} - \Lambda_{t+1}^{sh} \right] N_{t+1}^{sh} \frac{\partial P_{t+1}^{h}}{\partial N_{t+1}^{k}}, \end{aligned} \tag{33}$$

as the *susceptible* social wedge. The social wedge is a capital gain operating through the effect of having one more susceptible on reducing the probability of encountering an asymptomatic. Similarly, the fourth and fifth terms in the final column vector of(31) are also identical, pertaining to the effects of the measure of asymptomatics. This wedge,

$$\mathcal{W}_{t+1}^{a} = N_{t+1}^{T} \frac{\partial \Pi_{t+1}^{T}}{\partial N_{t+1}^{k}} \Lambda_{t+1}, \quad k = \{as, ai\} \tag{34}$$

$$\begin{aligned} =& \Big[(1 - \nu_{t+1}^{s\ell,sh}) \nu^{s\ell,sm} \Lambda_{t+1}^{sm} - \nu_{t+1}^{s\ell,sh} \Lambda_{t+1}^{sh} \Big] N_{t+1}^{s\ell} \frac{\partial P_{t+1}^{\ell}}{\partial N_{t+1}^{k}} \\ & + \left[\nu^{sm,as} \Lambda_{t+1}^{as} + \nu^{sm,ai} \Lambda_{t+1}^{ai} - (1 - \nu_{t+1}^{sm,sh}) \Lambda_{t+1}^{sm} - \nu_{t+1}^{sm,sh} \Lambda_{t+1}^{sh} \right] N_{t+1}^{sm} \frac{\partial P_{t+1}^{m}}{\partial N_{t+1}^{k}} \\ & + \left[\nu^{sh,as} \Lambda_{t+1}^{as} + \nu^{sh,ai} \Lambda_{t+1}^{ai} - \Lambda_{t+1}^{sh} \right] N_{t+1}^{sh} \frac{\partial P_{t+1}^{h}}{\partial N_{t+1}^{k}}, \end{aligned} \tag{35}$$

will be referred to as the *asymptomatic* social wedge; it is the capital loss due to the rise in the probability of encountering an asymptomatic individual due to an increase in the number of asymptomatics.

To see that the susceptible social wedge, $\mathcal{W}^s_{t+1}$, is a capital *gain* while the asymptomatic social wedge, $\mathcal{W}^a_{t+1}$, is a capital *loss*, notice that

$$\frac{\partial P^j_{t+1}}{\partial N^k_{t+1}} = \frac{\partial P^j_{t+1}}{\partial F_{t+1}} \frac{\partial F_{t+1}}{\partial N^k_{t+1}}, \quad k \in \{s\ell, sm, sh, as, ai\}, \quad j \in \{\ell, m, h\}. \tag{36}$$

The first term is the change in the probability of a susceptible-to-asymptomatic transition due to a change in the likelihood of a encountering an asymptomatic in a single encounter; the second term describes how this likelihood changes with a particular population measure. From (29), $\partial P^j_t / \partial F_t > 0$ is independent of the population measures. This partial derivative reflects the fact that the probability of a susceptible-to-asymptomatic transition increases with the probability of meeting an asymptomatic in a given meeting. Next, from (30), the frequency of meeting with an asymptomatic increases with the measure of asymptomatics, and decreases with the measure of susceptibles. Consequently, the sign of the second term in (36) differs between asymptomatics and susceptibles and so the two social wedges necessarily differ in sign.

Recalling that (known) infected individuals self isolate, the final entry in the last column vector in (31) is zero.

2.4 Firms

Each firm faces a static profit maximization problem,

$$\max_{\tilde{K}_t, \tilde{H}_t} F(\tilde{K}_t, \tilde{H}_t) - w_t \tilde{H}_t - r_t \tilde{K}_t$$

with

$$F(\tilde{K}_t, \tilde{H}_t) = \tilde{K}_t^{\theta} \tilde{H}_t^{1-\theta} \tag{37}$$

2.5 Market Clearing

The market clearing conditions are: labor market,

$$(N^{s\ell}_t + N^{sm}_t + N^{sh}_t + N^{as}_t + N^{ai}_t) H_t = \tilde{H}_t,$$

capital or asset market,

$$a_t = \tilde{K}_t,$$

and goods market,

$$(1 - N^i_t) C_t + N^i_t C^i_t + \tilde{K}_{t+1} = F(\tilde{K}_t, \tilde{H}_t) + (1 - \delta)\tilde{K}_t.$$

Table 1: Parameters

α^{ℓ}	0.0068	ω	1.9283	$\nu^{sh,as}$	0.2000
α^{m}	0.0137	ϕ	0.7012	$\nu^{as,s\ell}$	0.2000
α^{h}	0.0205	$\underline{s}$	0.0500	$\nu^{sm,as}$	0.4000
β	0.9999	θ	0.3000	$\nu^{ai,i}$	0.2000
δ	0.0002	$\nu^{s\ell,sm}$	0.0041	$\nu^{i,s\ell}$	0.0909
μ_c	0.5476	$\nu^{s\ell,sh}$	0.0001	ξ_1	4.7500
μ_h	24.0000	$\nu^{s\ell,as}$	0.6000	ξ_2	6312.1040
μ_s	40.0000	$\nu^{sm,sh}$	0.0001	ξ_3	2.0000

3 Calibration

The full set of parameters and their benchmark values are given in Table 1. The remainder of this section describes how these parameters were calibrated.

The discount factor, β, capital share, θ, depreciation, δ, and preference weights on leisure, ω, and social time, ϕ, are set so that in the non-pandemic steady state, the following conditions hold:

(1) Capital's share of income is 30%; see Gomme and Rupert (2007).

(2) The annual depreciation rate is 8%; again, see Gomme and Rupert (2007).

(3) The annual real interest rate is 4%, a common macroeconomic target.

(4) Hours worked are 25% of the time endowment.

(5) Social time is 20% of the time endowment.

In the non-pandemic steady state, capital is 4031.984 and consumption is 3.652. Given the non-pandemic steady state,

(1) μ_c is set so that there are 2 daily contacts due to consumption (shopping).

(2) μ_h is assigned a value so that working generates 6 daily contacts.

(3) μ_s delivers 8 daily contacts due to social time.

Next come pandemic-specific parameters. To discipline these choices, some of these parameters are calibrated to observations for the COVID-19 pandemic.

(1) $\underline{s}$, minimum social time, is set to 1/4 of non-pandemic social time.

(2) The average duration of the immunity boost following recovery from COVID-19 is about 8 months (2/3 of a year); see Stein et al. (2023) for a survey of the empirical evidence. With this in mind, $\nu^{s\ell,sm}$, the daily probability of transiting from susceptible-low to susceptible-medium, is assigned the value $\frac{1}{(2/3)365}$.

(3) The average duration of the asymptomatic phase of COVID is about 5 days (Anderson et al., 2020); thus, the probabilities of exiting the asymptomatic phase, $\nu^{ai,i}$ and $\nu^{as,s\ell}$, are set to 1/5.

(4) The average duration of the infected phase is around 11 days (Anderson et al., 2020), and so the probability of exiting this phase, $\nu^{i,s\ell}$, is assigned the value 1/11.

(5) So that there are *some* susceptible-high types in the pandemic steady state, the transition probabilities into this type, $\nu^{s\ell,sh}$ and $\nu^{sm,sh}$ are each assigned the value $1/10,000$.

(6) Given α^ℓ, the single contact probability that a susceptible-low contracts the virus, we set $\alpha^m = 2\alpha^\ell$ and $\alpha^h = 3\alpha^\ell$. These relative values reflect the progressively higher likelihood of the various susceptible types of catching the virus in a single meeting with an asymptomatic. The value of α^ℓ is determined by requiring that, in the model, daily new cases under the private planner corresponds to average daily new COVID-19 cases in the United States, 317,897 (taken from estimates by the Imperial College London from August 6, 2020 through December 25, 2022), relative to its population, 331,890,000. This evidence suggests that average daily new cases is close to 0.1% of the population.

(7) The type-specific probabilities that, upon contracting the virus, susceptible individuals are mild cases ($\nu^{s\ell,as}$, $\nu^{sm,as}$, and $\nu^{sh,as}$) are based on educated guesses that fewer than half of COVID cases are mild, and that the likelihood of severe COVID decreases with immunity ($\nu^{s\ell,as} > \nu^{sm,as} > \nu^{sh,as}$). These choices have very little influence on the epidemiological dynamics since *all* COVID cases pass through an asymptomatic phase.

(8) Recall that the daily utility cost of severe illness is $L = \xi_1 + \xi_2(N^i)^{\xi_3}$. This cost is assumed to be quadratic in the number of infected: $\xi_3 = 2$. In the private planner steady state, this cost is set to the utility value of $\overline{L}$ days' consumption in the non-pandemic steady state: $L = \overline{L}cU_1(c, \ell, s)$. Given that utility is logarithmic in consumption, the product of consumption with its marginal utility is one and so $L = \overline{L}$. How now to set the value of $\overline{L}$? For Sweden, Andersson et al. (2022) estimate that the welfare cost of social isolation is 9.1% of income. Assuming that this finding is equally applicable to

Americans, expressed in terms of consumption gives

$$\begin{aligned}\overline{L} &= 9.1\% \times \frac{\text{per capita GDP}}{\text{per capita consumption}} \\ &= 9.1\% \times \frac{\$77,178}{\$52,542} \\ &\simeq 0.134\end{aligned}$$

where per capita GDP and per capita consumption are for 2022.

Alternatively, we can use the probability of death and the value of a statistical life:

$$\begin{aligned}\overline{L} &= \frac{\text{value of a statistical life}}{\text{daily per capita consumption}} \times \frac{\text{case fatality rate}}{\text{average duration of illness}} \\ &= \frac{\$7,400,000}{\$31,046/365} \times \frac{1.1\%}{11} \\ &\simeq 87\end{aligned}$$

where the value of a statistical life is the one recommended by the US EPA in 2006, per capital consumption is similarly for 2006, and the case fatality rate is taken from Johns Hopkins University.

Finally, we can use the cost of a hospital stay due to COVID-19,

$$\begin{aligned}\overline{L} &= \frac{\text{daily cost of a hospital stay}}{\text{daily per capita consumption}} \\ &= \frac{\$11,275/11}{\$52,542/365} \\ &\simeq 7.12\end{aligned}$$

where the cost of a hospital stay is taken from Kapinos et al. (2024), the length of severe illness is 11 days as above, and per capita consumption is for 2022.

The value of isolation captures only a small part of the cost of a severe illness. To the extent that total COVID-19 cases are under-reported, the case fatality rate in the calculation based on the value of a statistical life is over-stated, and so is the value of $\overline{L}$. Not all (known) infected individuals end up in the hospital, and the cost of a hospital stay captures only part of the cost of illness. We set $\overline{L} = 5$ which is within the rather wide range of plausible values discussed above.

For the utility cost to increase with the fraction of the population infected requires $\xi_2 > 0$ and $\xi_1 < L$. With an eye to delivering "reasonable" numbers of infections, we set $\xi_1 = 0.95L$ and $\xi_2 = (L - \xi_1)/(N^i)^2$ where N^i is the steady state population share

of infected individuals. The social planner takes the values of ξ_1, ξ_2 and ξ_3, reported in Table 1, as given.

4 Steady States

This section discusses how the steady states differ across the two planners using the benchmark parameter values reported in Table 1. Relative to the non-pandemic steady state, both planners curtail socioeconomic activity. However, the social planner does so to a greater degree. Daily contacts serve as a convenient summary measure of overall socioeconomic activity. While the private planner reduces daily contacts by 1% compared to the non-pandemic steady state, the social planner reduces contacts by 7.2%. These differences can be traced directly to differences in the pandemic wedges between the two planners. Recalling that the pandemic wedge is the capital loss associated with an increase in daily contacts, the differences in the planners' pandemic wedges arise from the differences in their shadow values. In particular, under the social planner there are much larger gaps between the shadow values of susceptibles compared to asymptomatics, and so larger capital losses when susceptibles catch the virus. These larger gaps under the social planner can, in turn, be traced to the two social wedges associated with the transmission externalities which are only present under the social planner. Since the susceptible social wedge is the capital *gain* of more susceptibles while the asymptomatic social wedge is the capital *loss* of more asymptomatics, these social wedges lead to larger gaps between the shadow values of susceptibles versus asymptomatics, and so a larger pandemic wedge under the social planner.

Reduced socioeconomics under the social planner leads to fewer asymptomatic and infected individuals compared to the private planner. The social planner steady state is characterized by roughly 40% fewer individuals with the disease. These differences translate into a 40% lower likelihood of encountering an asymptomatic individual in a given contact. The reduced socioeconomic activity under the social planner sets off a sort of "virtuous circle" which operates through the transmission externality: reduced socioeconomic activity reduces daily contacts, thereby lowering the fraction of the population with the virus, which lessens the likelihood of encountering an asymptomatic individual, which further cuts the size of the population with the virus, and so on.

The rankings of the shadow values provide further insights into the model's mechanisms. From Table 2, the private planner's rankings can be summarized as:

$$\Lambda^{as} \simeq \Lambda^{s\ell} > \Lambda^{sm} > \Lambda^{sh} > \Lambda^{ai} \simeq \Lambda^{i}. \tag{38}$$

Table 2: Steady States

	Private Planner	Social Planner
Output	4.5283	4.3041
Capital (K or a)	3992.4191	3794.7712
Consumption, susceptible (c)	3.6162	3.4370
Consumption, infected (c^i)	3.6299	3.5244
Work hours (h)	0.2491	0.2362
Social time (s)	0.1971	0.1824
Number daily contacts (y)	15.8424	14.8477
Lifetime Utility (V)	−9155.7400	−9146.6175
Utility, susceptible	−0.9930	−1.0044
Utility, infected	−0.9104	−0.9399
Utility cost of infection	5.0000	4.8450
Shadow values		
Susceptible-low ($\Lambda^{s\ell}$)	−10248.9156	−10196.6449
Susceptible-medium (Λ^{sm})	−10253.8265	−10219.8808
Susceptible-high (Λ^{sh})	−10274.6281	−10325.5653
Asymptomatic-susceptible (Λ^{as})	−10248.7364	−10537.1472
Asymptomatic-infected (Λ^{ai})	−10312.0276	−10601.2109
Infected (Λ^{i})	−10312.2423	−10260.7445
Population shares (%)		
Susceptible-low ($N^{s\ell}$)	20.2537	12.6793
Susceptible-medium (N^{sm})	72.7070	76.4351
Susceptible-high (N^{sh})	5.9311	10.2124
Asymptomatic-susceptible (N^{as})	0.1929	0.1089
Asymptomatic-infected (N^{ai})	0.2861	0.1763
Infected (N^{i})	0.6293	0.3880
Frequency of meeting an asymptomatic (%)	0.4820	0.2863
Pandemic wedge ($\mathcal{W}^p$)	−0.0019	−0.0131
Susceptible social wedge ($\mathcal{W}^s$)		0.1957
Asymptomatic social wedge ($\mathcal{W}^a$)		−68.1576

The rankings of the three susceptible types reflect their differences in infection probabilities. Since asymptomatic-susceptibles cannot catch the virus and will not experience severe symptoms, the private planner slightly prefers this type over the susceptible-lows. The infected are ranked lowest since they bring no resources into the family and they suffer the cost of severe illness. The social planner's rankings are:

$$\Lambda^{s\ell} > \Lambda^{sm} > \Lambda^{i} > \Lambda^{sh} > \Lambda^{as} > \Lambda^{ai}. \tag{39}$$

The key differences in the rankings are that of the infected, and of the asymptomatic-susceptibles. These differences arise because the social planner accounts for the virus transmission externality while the private planner does not. Since the infected isolate and so no longer spread disease, the social planner ranks the infected relatively highly; the private planner ranks them last. Similarly, because the asymptomatic-susceptibles spread the virus, the social planner ranks this type second last; the private planner ranks this group first. To be sure, the social planner accounts for how the aggregate measure of infected individuals affects the infection cost externality, this effect is small relative to the transmission externality.

To evaluate the steady state welfare cost of the pandemic, find the value of Δc that solves

$$U(c^* - \Delta c, h^*, s^*) = (1 - N^i)U(c, \ell, s) + N^i \left[U(c^i, 1 - \underline{s}, \underline{s}) - L(N^i)\right]. \tag{40}$$

In (40), the left-hand side variables correspond to pre-pandemic steady state while the right-hand side is steady state utility under one of the planners. The differences in the steady state welfare cost is small: For the private planner, it is 3% of pre-pandemic output; for the social planner, 2.9%. From this, it follows that the *steady state* gains of the social planner's mitigation policies are rather small. The role of the cost externality can be evaluated by solving (40) using the social planner's socioeconomic variables and the private planner's value for L. Roughly 60% of the difference in the planners' welfare costs are due to this externality.

5 The Pandemic

The model starts on day 1 in the non-pandemic steady state. All individuals have the susceptible-high epidemiological status. On day 2, unexpectedly, it is known that 0.001% of the population is of each asymptomatic type; the measure of susceptible-high individuals correspondingly falls by 0.002%. The model is then solved for 11,000 days under perfect foresight as a two-point boundary problem using an extended path algorithm (Fair and

Taylor, 1983) with a 'no change' terminal condition on all variables. An advantage of this solution method is that the model is solved exactly and nonlinearly.

Events for the pandemic evolve rapidly over the first few hundred days, then take a considerable period of time to settle into steady state. In order to see what is occurring at short and long horizons, in Fig. 2 time is expressed as the natural logarithm of the number of days since the start of the pandemic.

The model dynamics under the two planners are broadly similar in large part due to the inherent dynamics of the SAIS model. For roughly the first month, there are rather few asymptomatic and infected individuals, and the susceptible-high population share remains very high. The pace of infections accelerates in the second month. For some time, a positive feedback loop prevails: More asymptomatics increases the likelihood of encountering an asymptomatic, raising susceptibles' virus-catching probability, leading to a growing asymptomatic population share. With a lag, the infected population share also starts rising. However, the overall shape of the pandemic differs between the two planners. Under the private planner, the population share of infected individuals reaches its zenith of 5% on day 92; the social planner delivers a much lower peak, 2.4%, nearly two weeks later, on day 105. In language that became familiar in 2020, the social planner more successfully flattens the curve. It is, perhaps, easier to see this curve flattening in Fig. 3(a) which aggregates daily new cases (those newly asymptomatic) to quarterly observations. Under the private planner, new cases rise sharply over the first half year, then fall. In contrast, the social planner's more stringent socioeconomic restrictions smooths out over time the number of new cases, resulting in fewer new cases over the first half year, but then more cases over the following year. This difference between the two planners is chiefly attributable to the cost externality: When the cost of infection is constant (the value of L fixed), the social planner chooses a path with a much larger peak in the population share of the infected (35.3% compared to 15.7% for the private planner) much earlier (day 80 versus day 93 under the private planner); see Fig. 4.

Following peak infections, the epidemiological dynamics deliver a rising population share of susceptible-lows. Again, the social planner delivers a lower peak (34.8% compared to 47.8% under the private planner) at a much later date (day 400, or just over 13 months, as opposed to day 241, or 8 months). Thereafter, the share of susceptible-lows declines while that of susceptible-mediums grows, reflecting the loss of the immunity boost associated with a recent case of the disease. Eventually, the model settles into a steady state with positive population share of all epidemiological statuses.

The evolution of the socioeconomic side of the model is driven largely, but not exclusively, by the pandemic wedge. On impact, the private planner's pandemic wedge goes from zero

Figure 2: The Pandemic: 2020 and Beyond

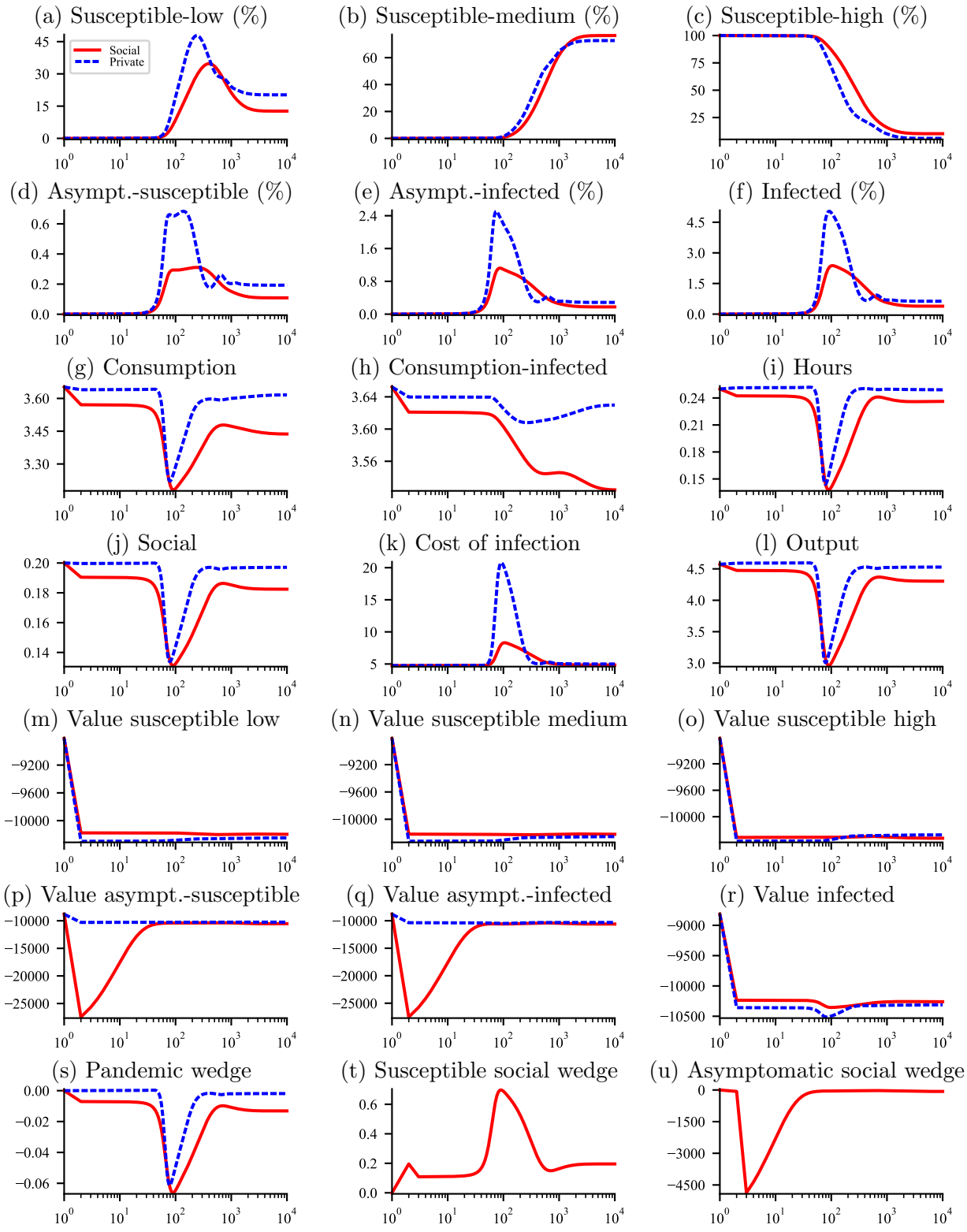

Figure 3: The Pandemic: Quarterly Data

(a) New Cases

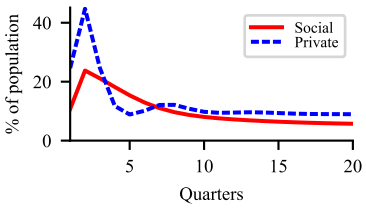

(b) Output

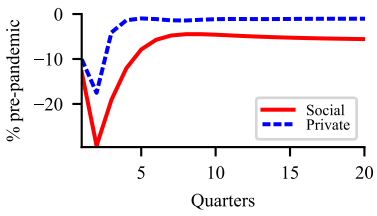

to a slightly *positive* value; in the pandemic steady state, its value is negative. Recall that the pandemic wedge captures the capital loss from an additional daily contact, with that additional daily contact fostering the virus spread and possibility of severe infections. Since there are initially no susceptible-low or susceptible-medium types, the change in the wedge is due to susceptible-high individuals becoming asymptomatic. For roughly the first $1\frac{1}{2}$ months, the shadow value of a susceptible-high is lower than the expected value of transiting to asymptomatic status. For the private planner, the shadow value of an asymptomatic-susceptible is close to that of a susceptible-low: asymptomatics contribute to family resources just like susceptibles, and the asymptomatic-susceptibles will shortly become susceptible-low while not suffering from severe illness. The shadow value of the asymptomatic-infected starts somewhat above that of the susceptible-high type before plunging as the utility cost of severe illness rises reflecting the increasing population share of infected individuals. It takes just over five weeks for the shadow value of the asymptomatic-infected types to pass below that of the susceptible-high types. Around the $1\frac{1}{2}$ month mark, the capital gain of a susceptible-high to asymptomatic transition switches to a capital loss, and the pandemic wedge is once more negative. From the Euler equations (18)–(21), by itself a positive pandemic wedge, $\mathcal{W}_t^p$, raises consumption, hours and social time. However, both the real wage, w_t, and the shadow value of income, λ_t, increase on day 2 which have the opposite effect on consumption and social time. The net effect is that on impact, consumption falls by 0.3%, social time by 0.2% while hours rise by 0.5%.

In contrast, the social planner's pandemic wedge immediately turns more negative. The huge capital loss when a susceptible-high transits to asymptomatic is largely due to the plunging shadow values of the asymptomatics. From (31), the social planner's shadow values are influenced by the two social wedges associated with the transmission externality. The shadow value of asymptomatics depends on the asymptomatic social wedge, $\mathcal{W}_{t+1}^a$, which captures the capital loss of an additional asymptomatic individual: More asymptomatics raise the measure of susceptible-to-asymptomatic transitions triggering capital losses since the

Figure 4: The Pandemic: Constant L

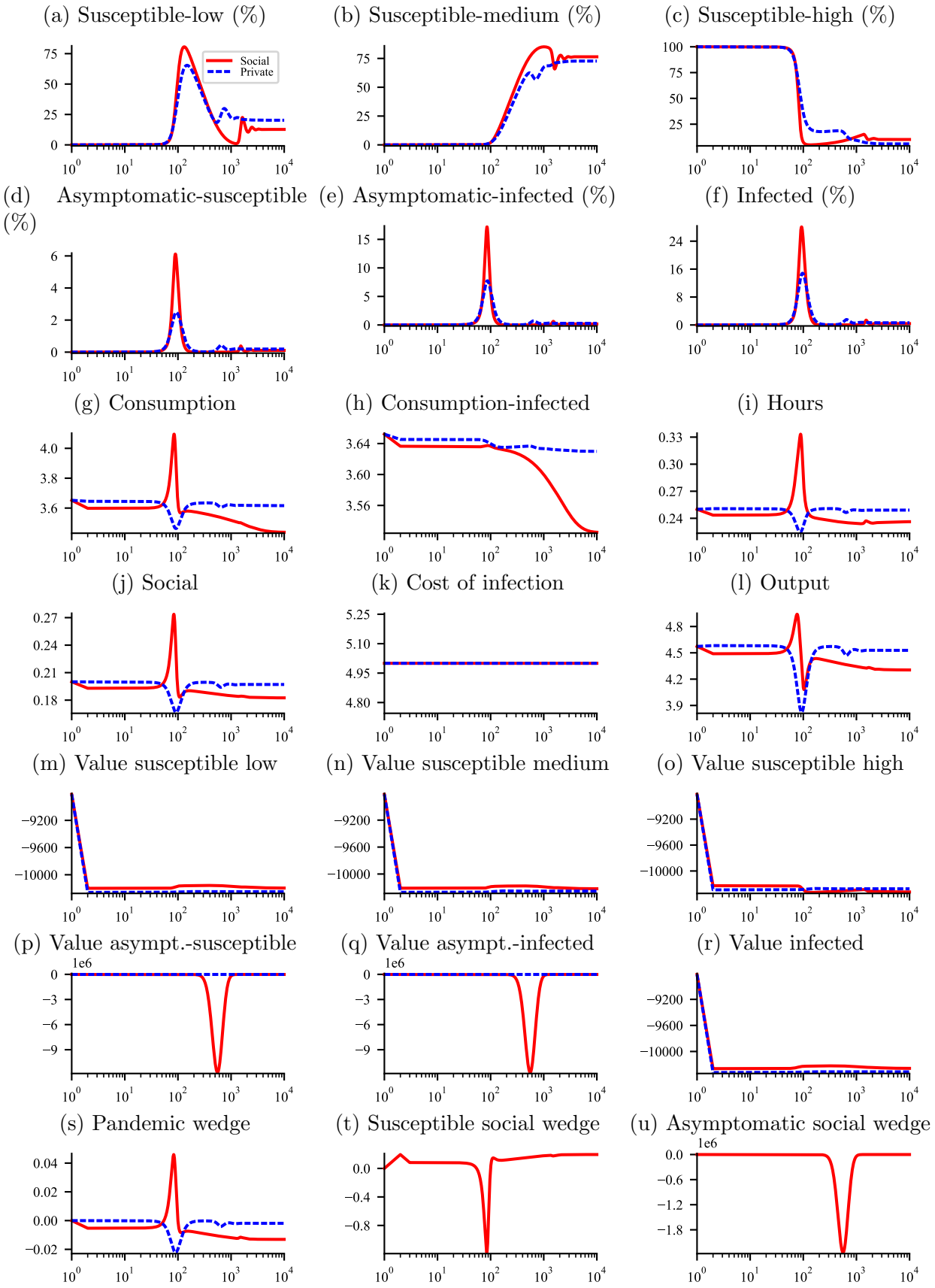

shadow value of susceptibles exceeds that of asymptomatics. The shadow value of asymptomatics on day 2 reflects the present value of these capital losses and so the very large drop in these shadow values. In a sense, the social planner assigns all of the future misery of being sick to the small measure of asymptomatics present on day 2. As the number of asymptomatics rises, the per-asymptomatic share of this misery falls. So, after the plunge, the shadow value of asymptomatics gradually rise. Chiefly due to the effects of the externalities, on impact the social planner reduces consumption by 2.2%, hours by 3.0%, and social time by 4.8%.

For a month or so, socioeconomic variables under the two planners do not change much. Over the subsequent two months, the social planner's choices for socioeconomic variables lie below those of the private planner – see Figs. 2(g), 2(i) and 2(j) – which accounts for the more gradual and delayed increase in the population shares of asymptomatic and infected individuals under the social planner. Again, the differences between the private and social planner solutions reflect the cost and transmission externalities. Once the asymptomatic population share starts rising more rapidly, both planners apply increasingly strict restrictions as dictated by their respective pandemic wedges. Indeed, the pandemic wedges reach their nadir just a few days after the peak of the asymptomatic population share. As the pandemic wedges approach their minimum, so does socioeconomic activity. The private planner's daily contacts drop from their pre-pandemic value of 16 to 10.6, a decline of 33.9%. The social planner reduces daily contacts a bit more: 10.3 or 35.6% lower than pre-pandemic levels.

Given the socioeconomic restrictions of the two planners, output is drastically impacted. At its worst, daily output under the private planner is 34.3% below the planner's steady state value; for the social planner, the decline is 35.3%. However, these are daily numbers. For the private planner, first quarter output is 10.2% below steady state; the second quarter, 17.4%; the third quarter, 4.1%; and subsequent quarters are within $1\frac{1}{2}\%$ of the pre-pandemic steady state. Output losses are larger and more prolonged under the social planner: 13.0% for the first quarter, 29.3% for the second, and 19.0% for the third. It is, perhaps, of interest that the output losses are largest *after* the asymptomatic and infected population shares peaked.

Of course, what matters is utility, not output. To give some idea of the magnitude of the welfare implications, consider the welfare costs of the pandemic relative to the pre-pandemic steady state. Specifically, solve for the value of Δc satisfying

$$\frac{U(c^* - \Delta c, \ell^*, s^*)}{1-\beta} = V \tag{41}$$

where the left-hand side variables are taken from the non-pandemic steady state, and V is

Figure 5: Assessing the Role of Socioeconomic Responses

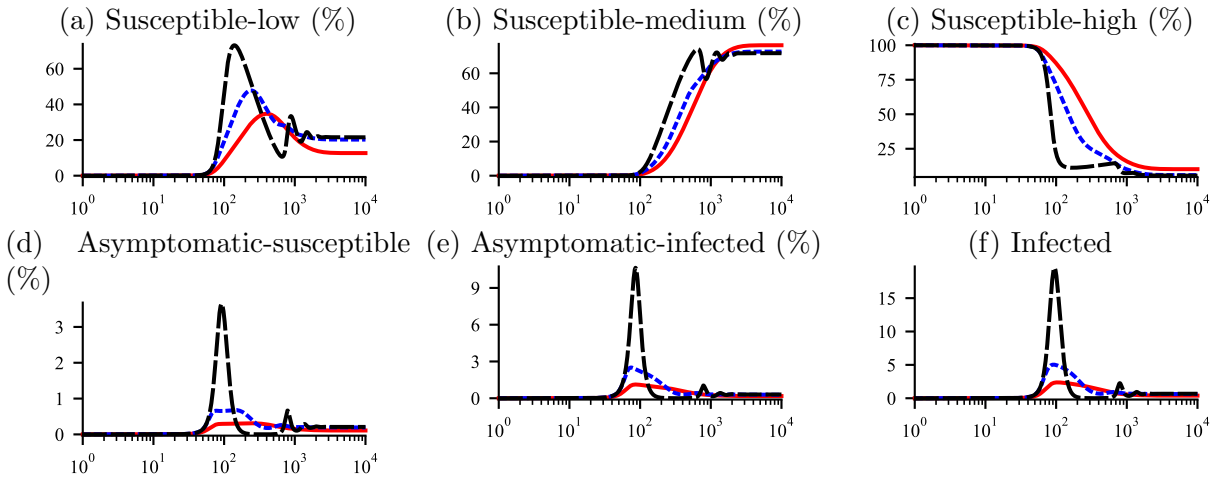

Note: Solid red, social planner; dashed blue, private planner; long-dashed black, no socioeconomic response.

lifetime utility of living through the pandemic. For the private planner,

$$V = \sum_{t=0}^{\infty} \beta^t \left\{ (1 - n_t^i) U(c_t, \ell_t, s_t) + n_t^i \left[U(c_t^i, 1 - \underline{s}, \underline{s}) - L(N_t^i) \right] \right\}; \tag{42}$$

the expression for the social planner differs only with respect to notation (uppercase letters replacing lowercase letters). By this metric, the welfare cost of the pandemic is 3.9% of pre-pandemic output for the private planner compared to 3.0% under the social planner. In other words, the social planner delivers a welfare gain of roughly 0.9% of pre-pandemic output relative to the private planner.

To assess the role of the socioeconomic responses to the pandemic, we solve the population dynamics holding daily contacts fixed at their pre-pandemic value of 16. For this exercise, we disregard the macroeconomic side of the model. Three interesting results emerge. First, as shown in Fig. 5, the peak population share of the (known) infected is 19.6%, much higher than either the private (5%) or social planner's (2.4%). The timing of the peak is within a few days of the private planner's. Second, there are endogenous waves. There is a second peak to the infected population share around day 800 (a little over two years) of 2.3% – nearly as high as the social planner's (first) peak. After 3¾ years, a smaller third wave crests with 0.95% of the population infected, although this value is close to the steady state share. Third, absent a socioeconomic response, the steady state population share of the infected is slightly higher: 0.7% compared to 0.6% under the private planner, and 0.4% for the social planner.

6 A New Variant of Concern

Viruses mutate over time, including those leading to pandemics like influenza or COVID-19. Of particular interest are *variants of concern* which are typically more contagious than the prevailing variant. As alluded to earlier, we model the introduction of such a new variant as shifting individuals in the model from lower levels of susceptibility to the highest, thereby making a large fraction of the population more likely to catch the virus in any given contact. Specifically, the model starts on day 1 in the pandemic steady state. On day 2, unexpectedly the probability of moving from susceptible-low or susceptible-medium to susceptible-high, $\nu^{sl,sh}$ and $\nu^{sm,sh}$, increase from 0.01% to 10% for 28 days (4 weeks), after which the probability returns to 0.01%. While this change in probability is unexpected, once this process starts, its future evolution is known and the model is again solved as a two-point boundary problem as described at the start of Section 5. This 28-day period is a proxy for the gradual geographic spread of a new variant in a model bereft of geography.

Fig. 6 shows that the population share of susceptible-high types reaches its apogee of nearly 90% on day 29, the last day on which the probability of moving to susceptible-high is elevated. As a consequence of the shift to high susceptibility, average susceptibility (average α) rises which causes the shares of the two asymptomatic pools to grow, followed by the size of the infected population. Like the pandemic scenario, the pinnacle of the infected population share is much lower under the social planner than the private planner: 2.3% versus 5%.

As with the pandemic scenario, the paths of the pandemic wedges – the capital losses of additional daily contacts – largely explain the evolution of the socioeconomic variables. Since the pandemic wedge grows in magnitude under both planners, both cut back on socioeconomic activity and daily contacts are abated to as little as 10.7 for the private planner (a reduction of 32.2%) and 10.5 for the social planner (a decline of 27.6% relative to steady state). Notice in Figs. 6(g), 6(i) and 6(j) that the social planner immediately cuts back on socioeconomic endeavors while the private planners' choices fall more gradually. Due to these socioeconomic restrictions, at its worst daily output is 32.5% below the private planner's steady state, and 30% below the social planner's steady state. As under the pandemic scenario, output losses are both more severe and longer lived under the social planner as shown in Fig. 6(l). After peak infections, the social planner more gradually returns to "normal" compared to the private planner which leads to a drawing out of the population shares of the asymptomatic and infected. The welfare cost of a new variant as measured using (41) and (42) is 3.6% of pre-pandemic output under the social planner and 4% under the private planner. In the case of a new variant, the social planner delivers a welfare gain of around

Figure 6: A New Variant of Concern

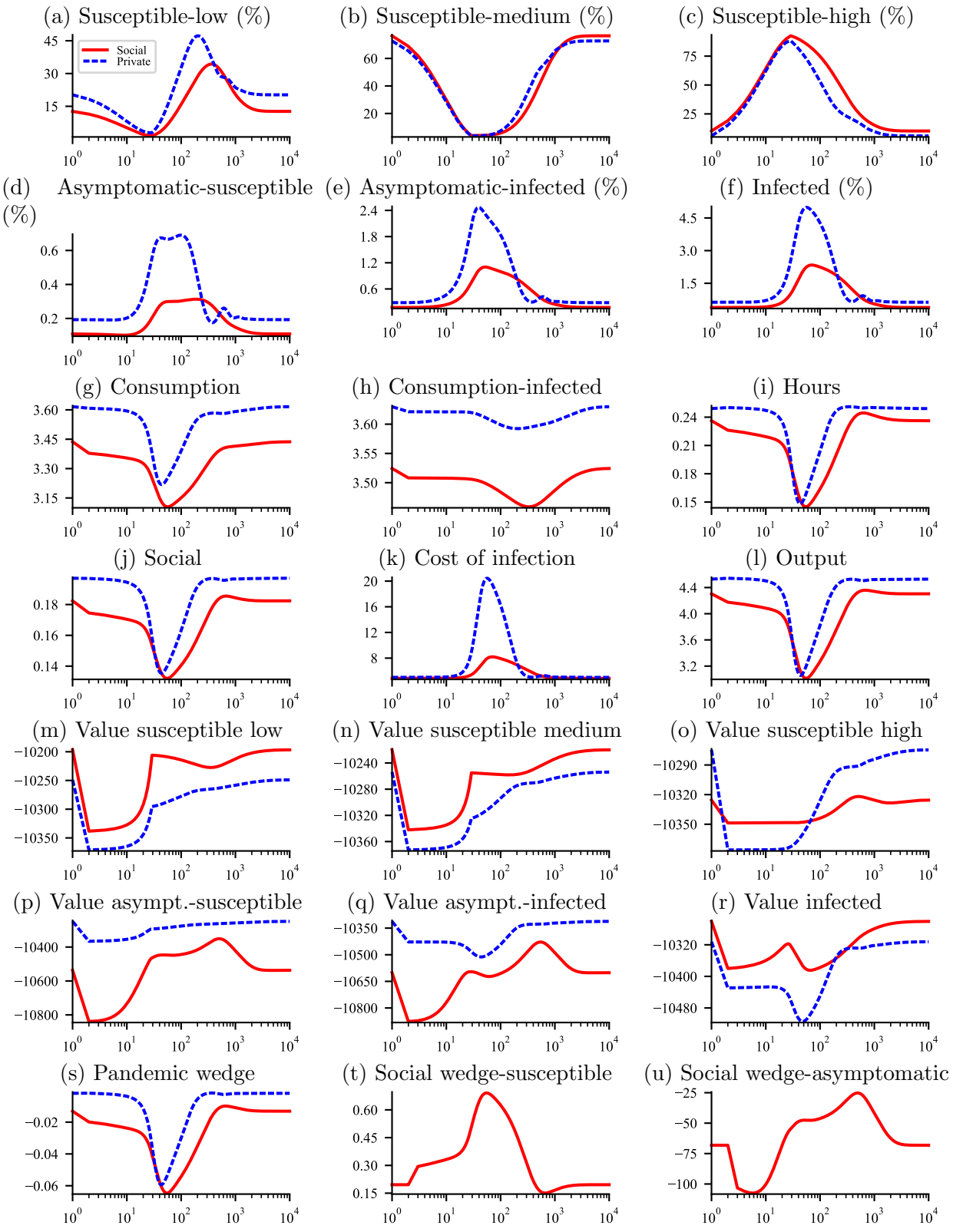

0.4% of pre-pandemic output.

7 Extensions

There are a number of possible extensions to our analysis. Arguably, the most glaring omission is vaccines. In the model, the only way for susceptible-high individuals to lower their susceptibility is to catch the virus, exposing themselves to the possibility of a bout of severe illness and its associated costs. Vaccines have played an important role after the first year of the US pandemic, either by reducing the chance of severe cases, or by lowering the likelihood of contracting COVID. Modeling vaccines would introduce a number of complications. To start, should the vaccinated be a fourth type of susceptible? There are several practical considerations. First, it takes time to recognize that a new variant of concern is circulating. Second, it takes weeks to manufacture the new vaccine. Third, it takes months to distribute the vaccine and administer doses; after all, it simply is not possible to vaccinate the entire US population on one day. How to model such time lags? With these delays, a new vaccine is unlikely to arrive before the peak of the asymptomatic population share at which point many of the benefits of a vaccine have dissipated. Finally, modeling vaccines would need to confront vaccine hesitancy. In early 2024, fewer than one in four adults in the US were vaccinated against the latest SARS-CoV-2 variant. Why?

We do not explicitly model mortality in the model. The utility cost of severe illness captures, in part, the losses associated with death. Including death would necessitate introducing births, otherwise the population would dwindle to nothing in the long run. Modeling these demographic issues within a utility-maximizing model is tough, raising a number of complex considerations.

Our analysis does not account for uncertainty – particularly that which prevailed early in the pandemic. At that time, the perception at least was that COVID was associated with high mortality rates; now, it is treated as a nuisance akin to the common cold or flu.

Since model individuals are infinitely lived, we cannot address age differences of a pandemic such as age-specific mortality risk. While COVID-19 disproportionately affected older individuals, earlier pandemics like the 1918-20 influenza pandemic had greater effects on the young. Absent prior information regarding the age effects of a future pandemic, introducing age differences is unlikely to affect our core policy prescriptions. Along similar lines, it is now known that children were not an important channel for spreading COVID-19 which suggests that the switch to remote learning did not substantially affect the course of the COVID-19 pandemic. In turn, remote learning had deleterious effects on schooling outcomes and social development of the young. Again, these facts are only known with hindsight and there is no

reason to believe that a future pandemic will have relatively benign effects on the young.

At best, our analysis accounts for mitigation measures like working from home and online shopping by calibrating the model to the US pandemic experience. Explicitly modeling such measures would necessitate explaining why some work is done in the office while other work can be performed at home. E-commerce sales in the US make up roughly 15% of total sales; what determines this fraction? Put differently, why do brick and mortar stores still exist?

The paths under the social planner in Section 5 are the socially optimal set of restrictions. Clearly, they do not resemble those that were actually put in place: immediate and drastic reductions in activities leading to daily contacts. Our model could be used to evaluate the welfare consequences of sub-optimal lockdown strategies. Such an exercise immediately runs into the issue that there was no single lockdown for the US. Instead, restrictions were, for the most part, set at the state level. A serious analysis would, then, need to account for not only these state differences in socioeconomic restrictions, but also for the contagion across state boundaries.

Regarding our calibration, the greatest parameter uncertainty surrounds those related to epidemiology: What are the appropriate values for the susceptible type-specific single contact infection probabilities (the αs)? What are the susceptible type-specific probabilities of ending up a severe case (the νs)? Our benchmark values for these parameters are educated guesses disciplined by US data on COVID cases. That said, it seems unlikely that better estimates of the αs and νs would substantially change our quantitative results, much less the underlying message concerning the differences between privately and socially optimal decisions.

8 Conclusion

We developed a tractable daily model combining epidemiology and macroeconomics, and the interactions between the two. There are two externalities in the model: the *cost externality* and the *transmission externality*. The cost externality, the daily cost of severe illness, was modeled as increasing in the population fraction of infected individuals. The transmission externality refers to how the susceptible-asymptomatic mix affects the likelihood of encountering an asymptomatic individual in the course of engaging in daily activity. We solved the model for a private planner who does not account for these externalities, and a social planner who does. Under both planners, a *pandemic wedge* distorts consumption, work hours, and social time away from their pre-pandemic values. This pandemic wedge corresponds to the capital loss due to an additional daily contact – the shadow value of susceptibles less that of asymptomatics multiplied by the rise in the infection probability of that added contact. As-

sociated with the transmission externality are the *susceptible social wedge* which captures the capital gains of an additional susceptible individual (lowering the probability of encountering an asymptomatic), and the *asymptomatic social wedge*, the capital loss of an additional asymptomatic individual (which raises the chance of meeting with an asymptomatic). For the social planner, the susceptible social wedge pushes up the shadow value of susceptibles while the asymptomatic social wedge depresses the shadow value of asymptomatics.

Under our pandemic scenario, the social planner responds sooner and more severely limits socioeconomic activity than the private planner. While the social planner's choices lead to more pronounced and protracted output losses, they also "flatten the curve": the peak of the infected population share is much lower which in turn, lessens the utility losses of severe illness cases. After the peak, the social planner continues to restrict socioeconomic endeavors which spreads out the dynamics of the asymptomatic and infected population shares. While the welfare costs of SARS-CoV-2 are substantial under both planners, they are smaller under the social planner. We find that the social planner delivers a welfare gain of 0.9% of pre-pandemic output relative to the private planner. These results point more generally to the potential welfare gains of socially optimal restrictions during a future pandemic.

A Online Appendix, Not for Publication

The "Long" Bellman Equations and Euler Equations

This not-for-publication appendix presents the Bellman equations and Euler equations for the planners' problems without the use of matrix algebra.

The private planner

$$
\begin{aligned}
V(a_t, n_t^{s\ell}, n_t^{sm}, n_t^{sh}, n_t^{as}, n_t^{ai}, n_t^{i}; \mathcal{S}_t) \equiv \max\Big\{ & (n_t^{s\ell} + n_t^{sm} + n_t^{sh} + n_t^{as} + n_t^{ai}) U(c_t, \ell_t, s_t) \\
& + n_t^i [U(c_t^i, 1-\underline{s}, \underline{s}) - L(N_t^i)] + \beta V(a_{t+1}, n_{t+1}^{s\ell}, n_{t+1}^{sm}, n_{t+1}^{sh}, n_{t+1}^{as}, n_{t+1}^{ai}, n_{t+1}^{i}; \mathcal{S}_{t+1}) \\
+\lambda_t \big[& w_t (n_t^{s\ell} + n_t^{sm} + n_t^{sh} + n_t^{as} + n_t^{ai}) h_t + R_t^k a_t \\
& - (n_t^{s\ell} + n_t^{sm} + n_t^{sh} + n_t^{as} + n_t^{ai}) c_t - n_t^i c_t^i - a_{t+1} \big] \\
+ \Lambda_t^{s\ell} & \Big[(1-P_t^{\ell})(1-\nu_t^{s\ell,sh})(1-\nu^{s\ell,sm}) n_t^{s\ell} + \nu^{as,s\ell} n_t^{as} + \nu^{i,s\ell} n_t^{i} - n_{t+1}^{s\ell} \Big] \\
+ \Lambda_t^{sm} & \Big[(1-P_t^{m})(1-\nu_t^{sm,sh}) n_t^{sm} + (1-P_t^{\ell})(1-\nu_t^{s\ell,sh}) \nu^{s\ell,sm} n_t^{s\ell} - n_{t+1}^{sm} \Big] \\
+ \Lambda_t^{sh} & \Big[(1-P_t^{h}) n_t^{sh} + (1-P_t^{\ell}) \nu_t^{s\ell,sh} n_t^{s\ell} + (1-P_t^{m}) \nu_t^{sm,sh} n_t^{sm} - n_{t+1}^{sh} \Big] \\
+ \Lambda_t^{as} & \big[(1-\nu^{as,s\ell}) n_t^{as} + P_t^{\ell} \nu^{s\ell,as} n_t^{s\ell} + P_t^{m} \nu^{sm,as} n_t^{sm} + P_t^{h} \nu^{sh,as} n_t^{sh} - n_{t+1}^{as} \big] \\
+ \Lambda_t^{ai} & \big[(1-\nu^{ai,i}) n_t^{ai} + P_t^{\ell} \nu^{s\ell,ai} n_t^{s\ell} + P_t^{m} \nu^{sm,ai} n_t^{sm} + P_t^{h} \nu^{sh,ai} n_t^{sh} - n_{t+1}^{ai} \big] \\
+ \Lambda_t^{i} & \big[(1-\nu^{i,s\ell}) n_t^{i} + \nu^{ai,i} n_t^{ai} - n_{t+1}^{i} \big] \Big\}
\end{aligned}
\tag{A.1}
$$

First-order conditions:

$$
\begin{aligned}
c_t: \quad & (1-n_t^i) \left[U_1(c_t, \ell_t, s_t) - \lambda_t \right] \\
& + \Big[\nu^{s\ell,as} \Lambda_t^{as} + \nu^{s\ell,ai} \Lambda_t^{ai} - (1-\nu_t^{s\ell,sh})(1-\nu^{s\ell,sm}) \Lambda_t^{s\ell} \\
& \qquad - (1-\nu_t^{s\ell,sh}) \nu^{s\ell,sm} \Lambda_t^{sm} - \nu_t^{s\ell,sh} \Lambda_t^{sh} \Big] \mu_c \frac{\partial P_t^{\ell}}{\partial y_t} n_t^{s\ell} \\
& + \left[\nu^{sm,as} \Lambda_t^{as} + \nu^{sm,ai} \Lambda_t^{ai} - (1-\nu_t^{sm,sh}) \Lambda_t^{sm} - \nu_t^{sm,sh} \Lambda_t^{sh} \right] \mu_c \frac{\partial P_t^{m}}{\partial y_t} n_t^{sm} \\
& + \left[\nu^{sh,as} \Lambda_t^{as} + \nu^{sh,ai} \Lambda_t^{ai} - \Lambda_t^{sh} \right] \mu_c \frac{\partial P_t^{h}}{\partial y_t} n_t^{sh} = 0
\end{aligned}
\tag{A.2}
$$

$$
c_t^i: \quad U_1(c_t^i, 1-\underline{s}, \underline{s}) - \lambda_t = 0 \tag{A.3}
$$

$$
\begin{aligned}
h_t: \quad & (1-n_t^i)\left[U_2(c_t,\ell_t,s_t)+\lambda_t w_t\right] \\
& + \Big[\nu^{s\ell,as}\Lambda_t^{as}+\nu^{s\ell,ai}\Lambda_t^{ai}-(1-\nu_t^{s\ell,sh})(1-\nu^{s\ell,sm})\Lambda_t^{s\ell} \\
& \quad -(1-\nu_t^{s\ell,sh})\nu^{s\ell,sm}\Lambda_t^{sm}-\nu_t^{s\ell,sh}\Lambda_t^{sh}\Big]\mu_h\frac{\partial P_t^{\ell}}{\partial y_t}n_t^{s\ell} \\
& + \left[\nu^{sm,as}\Lambda_t^{as}+\nu^{sm,ai}\Lambda_t^{ai}-(1-\nu_t^{sm,sh})\Lambda_t^{sm}-\nu_t^{sm,sh}\Lambda_t^{sh}\right]\mu_h\frac{\partial P_t^{m}}{\partial y_t}n_t^{sm} \\
& + \left[\nu^{sh,as}\Lambda_t^{as}+\nu^{sh,ai}\Lambda_t^{ai}-\Lambda_t^{sh}\right]\mu_h\frac{\partial P_t^{h}}{\partial y_t}n_t^{sh}=0
\end{aligned} \tag{A.4}
$$

$$
\begin{aligned}
s_t: \quad & (n_t^{sh}+n_t^{s\ell}+n_t^{as}+n_t^{ai})U_3(c_t,\ell_t,s_t) \\
& + \Big[\nu^{s\ell,as}\Lambda_t^{as}+\nu^{s\ell,ai}\Lambda_t^{ai}-(1-\nu_t^{s\ell,sh})(1-\nu^{s\ell,sm})\Lambda_t^{s\ell} \\
& \quad -(1-\nu_t^{s\ell,sh})\nu^{s\ell,sm}\Lambda_t^{sm}-\nu_t^{s\ell,sh}\Lambda_t^{sh}\Big]\mu_s\frac{\partial P_t^{\ell}}{\partial y_t}n_t^{s\ell} \\
& + \left[\nu^{sm,as}\Lambda_t^{as}+\nu^{sm,ai}\Lambda_t^{ai}-(1-\nu_t^{sm,sh})\Lambda_t^{sm}-\nu_t^{sm,sh}\Lambda_t^{sh}\right]\mu_s\frac{\partial P_t^{m}}{\partial y_t}n_t^{sm} \\
& + \left[\nu^{sh,as}\Lambda_t^{as}+\nu^{sh,ai}\Lambda_t^{ai}-\Lambda_t^{sh}\right]\mu_s\frac{\partial P_t^{h}}{\partial y_t}n_t^{sh}=0
\end{aligned} \tag{A.5}
$$

$$
a_{t+1}: \quad \beta V_1(a_{t+1},n_{t+1}^{s\ell},n_{t+1}^{sm},n_{t+1}^{sh},n_{t+1}^{as},n_{t+1}^{ai},n_{t+1}^{i};\mathcal{S}_{t+1})=\lambda_t \tag{A.6}
$$

$$
n_{t+1}^{s\ell}: \quad \beta V_2(a_{t+1},n_{t+1}^{s\ell},n_{t+1}^{sm},n_{t+1}^{sh},n_{t+1}^{as},n_{t+1}^{ai},n_{t+1}^{i};\mathcal{S}_{t+1})=\Lambda_t^{s\ell} \tag{A.7}
$$

$$
n_{t+1}^{sm}: \quad \beta V_3(a_{t+1},n_{t+1}^{s\ell},n_{t+1}^{sm},n_{t+1}^{sh},n_{t+1}^{as},n_{t+1}^{ai},n_{t+1}^{i};\mathcal{S}_{t+1})=\Lambda_t^{sm} \tag{A.8}
$$

$$
n_{t+1}^{sh}: \quad \beta V_4(a_{t+1},n_{t+1}^{s\ell},n_{t+1}^{sm},n_{t+1}^{sh},n_{t+1}^{as},n_{t+1}^{ai},n_{t+1}^{i};\mathcal{S}_{t+1})=\Lambda_t^{sh} \tag{A.9}
$$

$$
n_{t+1}^{as}: \quad \beta V_5(a_{t+1},n_{t+1}^{s\ell},n_{t+1}^{sm},n_{t+1}^{sh},n_{t+1}^{as},n_{t+1}^{ai},n_{t+1}^{i};\mathcal{S}_{t+1})=\Lambda_t^{as} \tag{A.10}
$$

$$
n_{t+1}^{ai}: \quad \beta V_6(a_{t+1},n_{t+1}^{s\ell},n_{t+1}^{sm},n_{t+1}^{sh},n_{t+1}^{as},n_{t+1}^{ai},n_{t+1}^{i};\mathcal{S}_{t+1})=\Lambda_t^{ai} \tag{A.11}
$$

$$
n_{t+1}^{i}: \quad \beta V_7(a_{t+1},n_{t+1}^{s\ell},n_{t+1}^{sm},n_{t+1}^{sh},n_{t+1}^{as},n_{t+1}^{ai},n_{t+1}^{i};\mathcal{S}_{t+1})=\Lambda_t^{i} \tag{A.12}
$$

Envelope theorem:

$$
a_t: \quad V_1(a_t,n_t^{s\ell},n_t^{sm},n_t^{sh},n_t^{as},n_t^{ai},n_t^{i};\mathcal{S}_t)=\lambda_t R_t^k \tag{A.13}
$$

$$
\begin{aligned}
n_t^{s\ell}: \quad & V_2(a_t,n_t^{s\ell},n_t^{sm},n_t^{sh},n_t^{as},n_t^{ai},n_t^{i};\mathcal{S}_t)=U(c_t,\ell_t,s_t)+\lambda_t\left[w_t h_t-c_t\right] \\
& + (1-P_t^{\ell})(1-\nu_t^{s\ell,sh})(1-\nu^{s\ell,sm})\Lambda_t^{s\ell}+(1-P_t^{\ell})(1-\nu_t^{s\ell,sh})\nu^{s\ell,sm}\Lambda_t^{sm} \\
& + (1-P_t^{\ell})\nu_t^{s\ell,sh}\Lambda_t^{sh}+P_t^{\ell}\nu^{s\ell,as}\Lambda_t^{as}+P_t^{\ell}\nu^{s\ell,ai}\Lambda_t^{ai}
\end{aligned} \tag{A.14}
$$

$$
\begin{aligned}
n_t^{sm}: \quad & V_3(a_t,n_t^{s\ell},n_t^{sm},n_t^{sh},n_t^{as},n_t^{ai},n_t^{i};\mathcal{S}_t)=U(c_t,\ell_t,s_t)+\lambda_t\left[w_t h_t-c_t\right] \\
& + (1-P_t^{m})(1-\nu_t^{sm,sh})\Lambda_t^{sm}+(1-P_t^{m})\nu_t^{sm,sh}\Lambda_t^{sh} \\
& + \nu^{sh,as}P_t^{m}\Lambda_t^{as}+\nu^{sh,ai}P_t^{m}\Lambda_t^{ai}
\end{aligned} \tag{A.15}
$$

$$
\begin{aligned}
n_t^{sh}: \quad & V_4(a_t, n_t^{s\ell}, n_t^{sm}, n_t^{sh}, n_t^{as}, n_t^{ai}, n_t^{i}; \mathcal{S}_t) = U(c_t, \ell_t, s_t) + \lambda_t \left[w_t h_t - c_t \right] \\
& \quad + (1 - P_t^h)\Lambda_t^{sh} + P_t^h \nu^{sh,as} \Lambda_t^{as} + P_t^h \nu^{sh,ai} \Lambda_t^{ai} \qquad (A.16) \\
n_t^{as}: \quad & V_5(a_t, n_t^{s\ell}, n_t^{sm}, n_t^{sh}, n_t^{as}, n_t^{ai}, n_t^{i}; \mathcal{S}_t) = U(c_t, \ell_t, s_t) + \lambda_t \left[w_t h_t - c_t \right] \\
& \quad + (1 - \nu^{as,s\ell})\Lambda_t^{as} + \nu^{as,s\ell} \Lambda_t^{s\ell} \qquad (A.17) \\
n_t^{ai}: \quad & V_6(a_t, n_t^{s\ell}, n_t^{sm}, n_t^{sh}, n_t^{as}, n_t^{ai}, n_t^{i}; \mathcal{S}_t) = U(c_t, \ell_t, s_t) + \lambda_t \left[w_t h_t - c_t \right] \\
& \quad + (1 - \nu^{ai,i})\Lambda_t^{ai} + \nu^{ai,i} \Lambda_t^{i} \qquad (A.18) \\
n_t^{i}: \quad & V_7(a_t, n_t^{s\ell}, n_t^{sm}, n_t^{sh}, n_t^{as}, n_t^{ai}, n_t^{i}; \mathcal{S}_t) = U(c_t^i, 1 - \underline{s}, \underline{s}) - L(N_t^i) - \lambda_t c_t^i \qquad (A.19) \\
& \quad + \nu^{i,s\ell} \Lambda_t^{s\ell} + (1 - \nu^{i,s\ell})\Lambda_t^{i} \qquad (A.20)
\end{aligned}
$$

Update:

$$
\begin{aligned}
\lambda_t &= \beta \lambda_{t+1} R_{t+1}^k \qquad (A.21) \\
\Lambda_t^{s\ell} &= \beta \Big\{ U(c_{t+1}, \ell_{t+1}, s_{t+1}) + \lambda_{t+1} \left[w_{t+1} h_{t+1} - c_{t+1} \right] \\
&\quad + (1 - P_{t+1}^{\ell})(1 - \nu_{t+1}^{s\ell,sh})(1 - \nu^{s\ell,sm}) \Lambda_{t+1}^{s\ell} + (1 - P_{t+1}^{\ell})(1 - \nu_{t+1}^{s\ell,sh}) \nu^{s\ell,sm} \Lambda_{t+1}^{sm} \qquad (A.22) \\
&\quad + (1 - P_{t+1}^{\ell}) \nu_{t+1}^{s\ell,sh} \Lambda_{t+1}^{sh} + P_{t+1}^{\ell} \nu^{s\ell,as} \Lambda_{t+1}^{as} + P_{t+1}^{\ell} \nu^{s\ell,ai} \Lambda_{t+1}^{ai} \Big\} \\
\Lambda_t^{sm} &= \beta \Big\{ U(c_{t+1}, \ell_{t+1}, s_{t+1}) + \lambda_{t+1} \left[w_{t+1} h_{t+1} - c_{t+1} \right] \\
&\quad + (1 - P_{t+1}^{m})(1 - \nu_{t+1}^{sm,sh}) \Lambda_{t+1}^{sm} + (1 - P_{t+1}^{m}) \nu_{t+1}^{sm,sh} \Lambda_{t+1}^{sh} \qquad (A.23) \\
&\quad + \nu^{sh,as} P_{t+1}^{m} \Lambda_{t+1}^{as} + \nu^{sh,ai} P_{t+1}^{m} \Lambda_{t+1}^{ai} \Big\} \\
\Lambda_t^{sh} &= \beta \Big\{ U(c_{t+1}, \ell_{t+1}, s_{t+1}) + \lambda_{t+1} \left[w_{t+1} h_{t+1} - c_{t+1} \right] \\
&\quad + (1 - P_{t+1}^{h}) \Lambda_{t+1}^{sh} + P_{t+1}^{h} \nu^{sh,as} \Lambda_{t+1}^{as} + P_{t+1}^{h} \nu^{sh,ai} \Lambda_{t+1}^{ai} \Big\} \qquad (A.24) \\
\Lambda_t^{as} &= \beta \left\{ U(c_{t+1}, \ell_{t+1}, s_{t+1}) + \lambda_{t+1} \left[w_{t+1} h_{t+1} - c_{t+1} \right] + (1 - \nu^{as,s\ell}) \Lambda_{t+1}^{as} + \nu^{as,s\ell} \Lambda_{t+1}^{s\ell} \right\} \qquad (A.25) \\
\Lambda_t^{ai} &= \beta \left\{ U(c_{t+1}, \ell_{t+1}, s_{t+1}) + \lambda_{t+1} \left[w_{t+1} h_{t+1} - c_{t+1} \right] + (1 - \nu^{ai,i}) \Lambda_{t+1}^{ai} + \nu^{ai,i} \Lambda_{t+1}^{i} \right\} \qquad (A.26) \\
\Lambda_t^{i} &= \beta \left\{ U(c_{t+1}^i, 1 - \underline{s}, \underline{s}) - L(N_t^i) - \lambda_{t+1} c_{t+1}^i + \nu^{i,s\ell} \Lambda_{t+1}^{s\ell} + (1 - \nu^{i,s\ell}) \Lambda_{t+1}^{i} \right\} \qquad (A.27)
\end{aligned}
$$

The Social Planner

The Euler equations that differ:

$$
\begin{aligned}
\Lambda_t^{s\ell} = \beta\Big\{ & U(C_{t+1}, L_{t+1}, S_{t+1}) + \lambda_{t+1}\left[w_{t+1}H_{t+1} - C_{t+1}\right] \\
& + (1 - P_{t+1}^{\ell})(1 - \nu_{t+1}^{s\ell,sh})(1 - \nu^{s\ell,sm})\Lambda_{t+1}^{s\ell} + (1 - P_{t+1}^{\ell})(1 - \nu_{t+1}^{s\ell,sh})\nu^{s\ell,sm}\Lambda_{t+1}^{sm} \\
& + (1 - P_{t+1}^{\ell})\nu_{t+1}^{s\ell,sh}\Lambda_{t+1}^{sh} + P_{t+1}^{\ell}\nu^{s\ell,as}\Lambda_{t+1}^{as} + P_{t+1}^{\ell}\nu^{s\ell,ai}\Lambda_{t+1}^{ai} \\
& + \Big[\nu^{s\ell,as}\Lambda_{t+1}^{as} + \nu^{s\ell,ai}\Lambda_{t+1}^{ai} - (1 - \nu_{t+1}^{s\ell,sh})(1 - \nu^{s\ell,sm})\Lambda_{t+1}^{s\ell} \\
& - (1 - \nu_{t+1}^{s\ell,sh})\nu^{s\ell,sm}\Lambda_{t+1}^{sm} - \nu_{t+1}^{s\ell,sh}\Lambda_{t+1}^{sh}\Big] N_{t+1}^{s\ell}\frac{\partial P_{t+1}^{\ell}}{\partial N_{t+1}^{s\ell}} \\
& + \left[\nu^{sm,as}\Lambda_{t+1}^{as} + \nu^{sm,ai}\Lambda_{t+1}^{ai} - (1 - \nu_{t+1}^{sm,sh})\Lambda_{t+1}^{sm} - \nu_{t+1}^{sm,sh}\Lambda_{t+1}^{sh}\right] N_{t+1}^{sm}\frac{\partial P_{t+1}^{m}}{\partial N_{t+1}^{s\ell}} \\
& + \left[\nu^{sh,as}\Lambda_{t+1}^{as} + \nu^{sh,ai}\Lambda_{t+1}^{ai} - \Lambda_{t+1}^{sh}\right] N_{t+1}^{sh}\frac{\partial P_{t+1}^{h}}{\partial N_{t+1}^{s\ell}}\Big\}
\end{aligned}
\tag{A.28}
$$

$$
\begin{aligned}
\Lambda_t^{sm} = \beta\Big\{ & U(C_{t+1}, L_{t+1}, S_{t+1}) + \lambda_{t+1}\left[w_{t+1}H_{t+1} - C_{t+1}\right] \\
& + (1 - P_{t+1}^{m})(1 - \nu_{t+1}^{sm,sh})\Lambda_{t+1}^{sm} + (1 - P_{t+1}^{m})\nu_{t+1}^{sm,sh}\Lambda_{t+1}^{sh} \\
& + \nu^{sh,as}P_{t+1}^{m}\Lambda_{t+1}^{as} + \nu^{sh,ai}P_{t+1}^{m}\Lambda_{t+1}^{ai} \\
& + \Big[\nu^{s\ell,as}\Lambda_{t+1}^{as} + \nu^{s\ell,ai}\Lambda_{t+1}^{ai} - (1 - \nu_{t+1}^{s\ell,sh})(1 - \nu^{s\ell,sm})\Lambda_{t+1}^{s\ell} \\
& - (1 - \nu_{t+1}^{s\ell,sh})\nu^{s\ell,sm}\Lambda_{t+1}^{sm} - \nu_{t+1}^{s\ell,sh}\Lambda_{t+1}^{sh}\Big] N_{t+1}^{s\ell}\frac{\partial P_{t+1}^{\ell}}{\partial N_{t+1}^{sm}} \\
& + \left[\nu^{sm,as}\Lambda_{t+1}^{as} + \nu^{sm,ai}\Lambda_{t+1}^{ai} - (1 - \nu_{t+1}^{sm,sh})\Lambda_{t+1}^{sm} - \nu_{t+1}^{sm,sh}\Lambda_{t+1}^{sh}\right] N_{t+1}^{sm}\frac{\partial P_{t+1}^{m}}{\partial N_{t+1}^{sm}} \\
& + \left[\nu^{sh,as}\Lambda_{t+1}^{as} + \nu^{sh,ai}\Lambda_{t+1}^{ai} - \Lambda_{t+1}^{sh}\right] N_{t+1}^{sh}\frac{\partial P_{t+1}^{h}}{\partial N_{t+1}^{sm}}\Big\}
\end{aligned}
\tag{A.29}
$$

$$
\begin{aligned}
\Lambda_t^{sh} = \beta\Big\{ & U(C_{t+1}, L_{t+1}, S_{t+1}) + \lambda_{t+1}\left[w_{t+1}H_{t+1} - C_{t+1}\right] \\
& + (1 - P_{t+1}^{h})\Lambda_{t+1}^{sh} + P_{t+1}^{h}\nu^{sh,as}\Lambda_{t+1}^{as} + P_{t+1}^{h}\nu^{sh,ai}\Lambda_{t+1}^{ai} \\
& - (1 - \nu_{t+1}^{s\ell,sh})\nu^{s\ell,sm}\Lambda_{t+1}^{sm} - \nu_{t+1}^{s\ell,sh}\Lambda_{t+1}^{sh}\Big] N_{t+1}^{s\ell}\frac{\partial P_{t+1}^{\ell}}{\partial N_{t+1}^{sh}} \\
& + \left[\nu^{sm,as}\Lambda_{t+1}^{as} + \nu^{sm,ai}\Lambda_{t+1}^{ai} - (1 - \nu_{t+1}^{sm,sh})\Lambda_{t+1}^{sm} - \nu_{t+1}^{sm,sh}\Lambda_{t+1}^{sh}\right] N_{t+1}^{sm}\frac{\partial P_{t+1}^{m}}{\partial N_{t+1}^{sh}} \\
& + \left[\nu^{sh,as}\Lambda_{t+1}^{as} + \nu^{sh,ai}\Lambda_{t+1}^{ai} - \Lambda_{t+1}^{sh}\right] N_{t+1}^{sh}\frac{\partial P_{t+1}^{h}}{\partial N_{t+1}^{sh}}\Big\}
\end{aligned}
\tag{A.30}
$$

$$\begin{aligned}\Lambda_t^{as} = \beta\Big\{ & U(C_{t+1}, L_{t+1}, S_{t+1}) + \lambda_{t+1}\left[w_{t+1}H_{t+1} - C_{t+1}\right] + (1-\nu^{as,s\ell})\Lambda_{t+1}^{as} + \nu^{as,s\ell}\Lambda_{t+1}^{s\ell} \\ & + \Big[(1-\nu_{t+1}^{s\ell,sh})\nu^{s\ell,sm}\Lambda_{t+1}^{sm} - \nu_{t+1}^{s\ell,sh}\Lambda_{t+1}^{sh}\Big] N_{t+1}^{s\ell}\frac{\partial P_{t+1}^{\ell}}{\partial N_{t+1}^{as}} \\ & + \left[\nu^{sm,as}\Lambda_{t+1}^{as} + \nu^{sm,ai}\Lambda_{t+1}^{ai} - (1-\nu_{t+1}^{sm,sh})\Lambda_{t+1}^{sm} - \nu_{t+1}^{sm,sh}\Lambda_{t+1}^{sh}\right] N_{t+1}^{sm}\frac{\partial P_{t+1}^{m}}{\partial N_{t+1}^{as}} \\ & + \left[\nu^{sh,as}\Lambda_{t+1}^{as} + \nu^{sh,ai}\Lambda_{t+1}^{ai} - \Lambda_{t+1}^{sh}\right] N_{t+1}^{sh}\frac{\partial P_{t+1}^{h}}{\partial N_{t+1}^{as}}\Big\}\end{aligned} \tag{A.31}$$

$$\begin{aligned}\Lambda_t^{ai} = \beta\Big\{ & U(C_{t+1}, L_{t+1}, S_{t+1}) + \lambda_{t+1}\left[w_{t+1}H_{t+1} - C_{t+1}\right] + (1-\nu^{ai,i})\Lambda_{t+1}^{ai} + \nu^{ai,i}\Lambda_{t+1}^{i} \\ & + \Big[(1-\nu_{t+1}^{s\ell,sh})\nu^{s\ell,sm}\Lambda_{t+1}^{sm} - \nu_{t+1}^{s\ell,sh}\Lambda_{t+1}^{sh}\Big] N_{t+1}^{s\ell}\frac{\partial P_{t+1}^{\ell}}{\partial N_{t+1}^{ai}} \\ & + \left[\nu^{sm,as}\Lambda_{t+1}^{as} + \nu^{sm,ai}\Lambda_{t+1}^{ai} - (1-\nu_{t+1}^{sm,sh})\Lambda_{t+1}^{sm} - \nu_{t+1}^{sm,sh}\Lambda_{t+1}^{sh}\right] N_{t+1}^{sm}\frac{\partial P_{t+1}^{m}}{\partial N_{t+1}^{ai}} \\ & + \left[\nu^{sh,as}\Lambda_{t+1}^{as} + \nu^{sh,ai}\Lambda_{t+1}^{ai} - \Lambda_{t+1}^{sh}\right] N_{t+1}^{sh}\frac{\partial P_{t+1}^{h}}{\partial N_{t+1}^{ai}}\Big\}\end{aligned} \tag{A.32}$$

$$\Lambda_t^{i} = \beta\left\{U(C_{t+1}^{i}, 1-\underline{s}, \underline{s}) - L(N_t^i) - N_t^i L'(N_t^i) - \lambda_{t+1}c_{t+1}^{i} + \nu^{i,s\ell}\Lambda_{t+1}^{s\ell} + (1-\nu^{i,s\ell})\Lambda_{t+1}^{i}\right\} \tag{A.33}$$

References

Anderson, R. M., H. Heersterbeek, D. Klinkenberg, and T. D. Hollingsworth (2020). "How will country-based mitigation measures influence the course of the COVID-19 epidemic?" *The Lancet*.

Andersson, Ola, Pol Campos-Mercade, Fredrik Carlsson, Florian H. Schneider, and Erik Wengström (2022). "The Impact of Stay-at-Home Policies on Individual Welfare". *The Scandinavian Journal of Economics* 124 (2), pp. 340–362. eprint: https://onlinelibrary.wiley.com/doi/pdf/10.1111/sjoe.12470.

Atkeson, Andrew G. (2020). "On Using SIR Models to Model Disease Scenarios for COVID-19". *Federal Reserve Bank of Minneapolis Quarterly Review* 41 (1), pp. 1–33.

Bonnet, Gabrielle, Carl A.B. Pearson, Sergio Torres-Rueda, Francis Ruiz, Jo Lines, Mark Jit, Anna Vassall, and Sedona Sweeney (2024). "A Scoping Review and Taxonomy of Epidemiological-Macroeconomic Models of COVID-19". *Value in Health* 27 (1), pp. 104–116.

Eichenbaum, Martin S, Sergio Rebelo, and Mathias Trabandt (2021). "The Macroeconomics of Epidemics". *The Review of Financial Studies* 34 (11), pp. 5149–5187. eprint: https://academic.oup.com/rfs/article-pdf/34/11/5149/40724161/hhab040.pdf.

Fair, Ray and John Taylor (1983). "Solution and Maximum Likelihood Estimation of Dynamic Nonlinear Rational Expectations Models". *Econometrica* 51 (4), pp. 1169–1185.

Gainnitsarou, Chryssi, Stephen Kissler, and Flavio Toxvaerd (2021). "Waning Immunity and the Second Wave: Some Projections for SARS-CoV-2". *American Economic Review: Insights* 3 (3), pp. 321–338.

Gomme, Paul and Peter Rupert (2007). "Theory, Measurement, and Calibration of Macroeconomic Models". *Journal of Monetary Economics* 54 (2), pp. 460–497.

Kapinos, Kandice A., Richard M. Peters Jr., Robert E. Murphy, Samuel F. Hohmann, Ankita Podichetty, and Raymond S. Greenberg (2024). "Inpatient Costs of Treating Patients With COVID-19". *JAMA Network Open* 7 (1).

Stein, Caroline, Hasan Nassereldine, Reed J.D. Sorensen, Joanne O. Amlag, Catherine Bisignano, Sam Byrne, Emma Castro, Kaleb Coberly, James K. Collins, Jeremy Dalos, Farah Daoud, Amanda Deen, Emmanuela Gakidou, John R. Giles, Erin N. Hulland, Bethany M. Huntley, Kasey E. Kinzel, Rafael Lozano, Ali H. Mokdad, Tom Pham, David M. Pigott, Robert C. Reiner Jr., Theo Vos, Simon I. Hay, Christopher J.L.Murray, and Stephen S. Lim (2023). "Past SARS-CoV-2 Infection Protection Against Re-infection: A Systematic Review and Meta-analysis". *The Lancet* 401, pp. 833–842.